Design, economical synthesis and antiplasmodial evaluation of vanillin derived allylated chalcones and their marked synergism with artemisinin against chloroquine resistant strains…

ARTICLE *in* EUROPEAN JOURNAL OF MEDICINAL CHEMISTRY · MARCH 2014

Impact Factor: 3.45 · DOI: 10.1016/j.ejmech.2014.03.079

European Journal of Medicinal Chemistry 79 (2014) 350–368

Contents lists available at ScienceDirect

European Journal of Medicinal Chemistry

journal homepage: http://www.elsevier.com/locate/ejmech

Original article

Design, economical synthesis and antiplasmodial evaluation of vanillin derived allylated chalcones and their marked synergism with artemisinin against chloroquine resistant strains of *Plasmodium falciparum*☆

Nandini Sharma [a,1,2], Dinesh Mohanakrishnan [b,2], Upendra Kumar Sharma [a,1], Rajesh Kumar [a], Richa [a], Arun Kumar Sinha [a,c,*], Dinkar Sahal [b,**]

[a] Natural Plant Products Division, CSIR-Institute of Himalayan Bioresource Technology, Palampur 176061, HP, India
[b] Malaria Research Laboratory, International Centre for Genetic Engineering and Biotechnology, Aruna Asaf Ali Marg, New Delhi 110067, India
[c] Medicinal and Process Chemistry Division, CSIR-Central Drug Research Institute, Lucknow 226031, UP, India

ARTICLE INFO

Article history:
Received 22 November 2013
Received in revised form
24 March 2014
Accepted 27 March 2014
Available online 1 April 2014

Keywords:
Plasmodium falciparum
Allylated chalcones
Chloroquine
Artemisinin
Synergism

ABSTRACT

The *in vitro* blood stage antiplasmodial activity of a series of allylated chalcones based on the licochalcone A as lead molecule was investigated against chloroquine (**CQ**) sensitive *Pf*3D7 and **CQ** resistant *Pf*INDO strains of *Plasmodium falciparum* using SYBR Green I assay. Of the forty two chalcones tested, eight showed $IC_{50} \leq 5$ μM. Structure–activity relationship (SAR) studies revealed **9** {1-(4-Chlorophenyl)-3-[3-methoxy-4-(prop-2-en-1-yloxy)phenyl]-prop-2-en-1-one} as the most potent (IC_{50}: 2.5 μM) against *Pf*3D7 with resistance indices of 1.2 and 6.6 against *Pf*Dd2 and *Pf*INDO strains, respectively. Later on, the synergistic effects **9** with standard antimalarials {artemisinin (**ART**) and chloroquine (**CQ**)} were studied in order to provide the basis for the selection of the best partner drug. *In vitro* combinations of **9** with **ART** showed strong synergy against *Pf*INDO (ΣFIC_{50}: 0.31–0.72) but additive to slight antagonistic effects (ΣFIC_{50}: 1.97–2.64) against *Pf*3D7. ΣFIC_{50} 0.31 of **ART**+**9** combination corresponded to a 320 fold and 3 fold reduction in IC_{50} of **9** and **ART**, respectively. Similar combinations of **9** with **CQ** showed synergy to additivity to mild antagonism against the two strains {ΣFIC_{50}: 0.668–2.269 (*Pf*INDO); 1.45–2.83 (*Pf*3D7)}. Drug exposure followed by drug withdrawal indicated that **9** taken alone at IC_{100} killed rings, trophozoites and schizonts of *P. falciparum*. The combination of **ART** and **9** (1X ΣFIC_{100}) selectively inhibited the growth of rings while the 2X ΣFIC_{100} combination of the same caused killing of rings without affecting trophozoites and schizonts. In contrast, the 1X combination of **CQ** and **9** (ΣFIC_{100}: 0.5) killed rings and trophozoites. DNA fragmentation and loss of mitochondrial membrane potential ($\Delta\Psi m$) in the **9** treated *P. falciparum* culture indicated apoptotic death in malaria parasites. Prediction of ADME properties revealed that most of the molecules did not violate Lipinski's parameters and have low TPSA value suggesting good absorption. The results suggest the promising drug-like properties of **9** against **CQ** resistant *Pf* and propensity for synergy with classical antimalarial drugs together with easy and economical synthesis.

1. Introduction

Despite years of continual efforts for its eradication, malaria that kills approximately three million people per annum [1,2] still remains a globally prevalent parasitic disease. Almost all these deaths are caused by *Plasmodium falciparum*, one of the four species of malaria parasites in humans [2]. The principal reason hampering malaria control is the emergence of resistance by *P. falciparum* strains to the first-line antimalarial drugs like chloroquine [3,4].

Abbreviations: SAR, Structure–activity relationship; CQ, Chloroquine; ART, Artemisinin; Pf, *Plasmodium falciparum*.

☆ IHBT and CDRI Communication No: 2387/8653.

* Corresponding author. Present address: Medicinal and Process Chemistry Division, CSIR-CDRI, Lucknow, UP, India.
** Corresponding author: Malaria Research Laboratory, International Centre for Genetic Engineering and Biotechnology, New Delhi, India
E-mail addresses: aksinha08@rediffmail.com (A.K. Sinha), dinkar@icgeb.res.in (D. Sahal).
[1] Present address: Department of Chemistry, Katholieke Universiteit Leuven, Celestijnenlaan 200F, B-3001 Leuven, Belgium.
[2] Equal contributions.

http://dx.doi.org/10.1016/j.ejmech.2014.03.079
0223-5234/

Natural products have always remained in focus for the discovery of new drug leads intended for the treatment of human diseases [5]. The major breakthroughs in the use of natural products as antimalarials are the discoveries of quinine [6] and artemisinin [7]. At present, artemisinin is the most effective treatment for curing chloroquine-resistant *P. falciparum* infections [6–9]; however its indiscriminate use as monotherapy has raised the concern of emergence of drug resistance [10–14]. To slow down the resistance to this vital class of drugs; artemisinin based combination therapies (ACTs) are being advocated by WHO [15]. This should also lessen pressure on the rising demand for artemisinin-a natural product in short supply and with commercially unviable synthesis [16]. Further, this urgent need to develop new antimalarial agents or drug combinations that are effective and support treatment at affordable cost is supplemented by the recent emergence of resistance against ACTs manifested in the form of delayed parasite clearance [17].

In the light of this perspective, natural products or their synthetic derivatives as a partner compound are an attractive search option for novel ACTs. One such important class of natural compounds is 1,3-diarylprop-2-en-1-ones, commonly termed as chalcones. The appeal of working with chalcones stems from their synthetic accessibility, the various ways the core structure can be diversified depending on the substitution patterns on the two aromatic rings and their ability to confer drug-like properties to compound libraries modeled on them [18]. Chalcones drew the attention of chemists when licochalcone A (a 1,1-dimethyl allylated natural product) isolated from Chinese liquorice roots, was reported to exhibit potent *in vivo* and *in vitro* antimalarial activity against both chloroquine-susceptible and chloroquine-resistant *P. falciparum* strains [19]. Since then, several natural chalcones such as xanthohumol, 5-prenylbutein, licoagrochalcone A, homobutein and crotaorixin have been reported to exhibit *in vitro* antiplasmodial activity against *P. falciparum* strains with IC_{50} values in the range 10.3–16.1 μM [20–22]. However, limitations such as low percentage in natural resources, toxicity [23], low bioavailability, poor solubility and tedious total synthesis have generally restrained their use in humans [22,23]. Nevertheless, the compounds described above provide useful synthons for semi-synthetic transformations of easily available precursors into newer and modified antimalarials [24–29] against not only drug-sensitive, but also drug-resistant strains of *Plasmodium*. In this context, an analogue of licochalcone A, 2,4-dimethoxy-4′-butoxychalcone was found to exhibit potent activity against *P. falciparum in vitro* and the rodent parasites *Plasmodium berghei* and *Plasmodium yoelii in vivo* [23].

A close scrutiny of natural antimalarial chalcones has revealed that a vast majority of these possess substituted allylated aromatic rings (prenyl or geranyl group) as important elements of their pharmacophores. The importance of prenyl or allyl group for enhancing the bioactivities of flavonoids and chalcones is well documented in literature [22,30–33]. Furthermore, the prenyl moiety contributes to the lipophilicity of the molecule, an important requirement for antimalarial activity [34]. However, its incorporation needs tedious multi-step synthesis and hence could be replaced by groups with comparable lipophilic characters involving economical synthons without any decrease in antimalarial activity.

Here we report the design, synthesis and *in vitro* antiplasmodial evaluation of forty-two allylated chalcones which are structurally similar to natural licochalcone A. To address the demands of green chemistry [35], vanillin [36] – an easily available natural precursor [37], has been utilized for the synthesis of these chalcones. The chalcones under study are divided into four main types according to the substitution of ring A: (i) *C*-allylated, (ii) *O*-allylated, (iii) both *C*- and *O*-allylated, and (iv) *O*-diallylated. First, we have examined the antiplasmodial structure activity relationship (SAR) of all allylated chalcones. Next, we have studied the antiplasmodial effect of the combinations of one of the most potent allylated chalcones i.e. **9** with chloroquine and artemisinin against **CQ** sensitive (*Pf*3D7) and resistant (*Pf*INDO) strains of *P. falciparum*. Finally, we studied the mechanistic features of the antiplasmodial action of **9** by microscopic evaluation of stage specific activity, kill kinetics and mode of cell death by using fluorescent and non-fluorescent staining methods against erythrocytic stages of *P. falciparum* which indicated that **9** induce apoptotic cell death. Also, combination of **9** with **ART** exhibits strong synergy against a highly **CQ** resistant strain of *P. falciparum*.

2. Results and discussion

2.1. Chemistry

The synthesis of allylated chalcones is summarized in Schemes 1–5. 4-allyloxy-3-methoxybenzaldehyde (**1b**) was obtained by refluxing vanillin (**1a**) with allyl bromide in the presence of K_2CO_3 [38,39]. Compound **1b** upon microwave irradiation at 200 °C underwent Claisen reaction to yield **2b** which was transformed into **3b** using dimethyl sulfate as methylating agent [40,41] and into **4b** by reacting with allyl bromide [40]. Claisen–Schmidt condensation of **1a** and **1b**–**4b** with the corresponding acetophenones [42,43] gave chalcones (**1**–**19**) which were purified by chromatography and crystallization (Scheme 1).

Similarly, 4-allyloxyacetophenone (**5b**), obtained by reacting 4-hydroxyacetophenone (**2a**) with allyl bromide [38] was condensed with **1b** to give corresponding chalcone **20**. Likewise, corresponding allyloxy benzaldehydes (**6b**, **7b**) were obtained by refluxing 2-hydroxy-3-methoxybenzaldehyde (**3a**) and 3-hydroxy-4-methoxybenzaldehyde (**4a**), respectively with allyl bromide in the presence of K_2CO_3 in dry acetone [38,39]. Compounds **6b** and **7b** upon Claisen–Schmidt condensation with 4-chloroacetophenone in the presence of aqueous NaOH [42,43] gave chalcones (**21** and **22**) which were purified by chromatography and crystallization (Scheme 2). Similarly, **23** obtained by condensation of **1a** with chloroacetophenone [42,43]. **23** upon reaction with prenyl bromide, 1-butyl bromide and 4-bromobenzyl bromide yielded **24**–**26**, respectively [39] (Scheme 3).

In a similar vein, analogues of vanillin, such as syringaldehyde (**5a**), 4-hydroxybenzaldehyde (**6a**), 2-hydroxybenzaldehyde (**7a**), 3-ethoxy-4-hydroxybenzaldehyde (**8a**) and 3,4-dihydroxybenzaldehyde (**9a**) were reacted with allyl bromide [38,39] to provide *O*-allylated benzaldehydes (**8b**–**12b**). Compounds **8b**–**12b** upon Claisen–Schmidt condensation with 4-chloroacetophenone gave chalcone products (**27**–**31**). Similarly, 4-allyloxy-3-methoxyacetophenone (**13b**) was obtained by reaction of 4-hydroxy-3-methoxyacetophenone (**10a**) with allyl bromide which on condensation with 4-chlorobenzaldehyde provided chalcone **32**. **14b** was obtained by reaction of 2,4-dihydroxyacetophenone (**11a**) with allyl bromide in the presence of K_2CO_3 [42,43] (Scheme 4).

Chalcones **33**–**38** were prepared by reacting **1b** with various heteroaromatic acetophenones (Scheme 5) as incorporation of heteroatom generally increases the biological activities. Hence, compound **39** was synthesized by reaction of **18** with 4,7-dichloroquinoline in THF in the presence of K_2CO_3 [44] which upon further reaction with allyl bromide in the presence of KOH and THF yielded **40**. Compounds **41** and **42** were prepared by refluxing **9** with phenylhydrazine [45] and guanidine hydrochloride [46], respectively (Scheme 5).

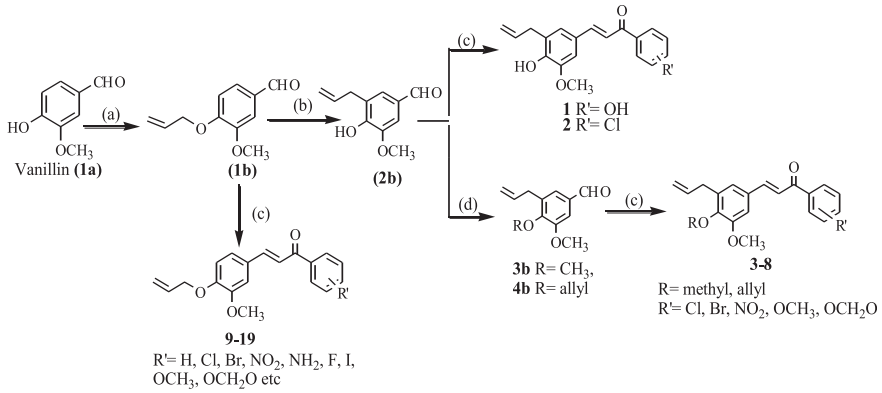

Scheme 1. Synthesis of *C* & *O*-allylated chalcones **1**–**19** containing vanillin as a core structure on ring A. Reagents and conditions: (a) allyl bromide, potassium carbonate, anhydrous acetone, reflux; (b) MW at $T = 200$ °C for 10 min; (c) 10% aq. NaOH, methanol, substituted acetophenone, stir at rt; (d) dimethyl sulfate, NaOH, stir at rt; or allyl bromide, K_2CO_3 and anhydrous acetone, reflux.

2.2. Biological activity

Several reports highlighting the importance of *O*-alkylated group on ring B (predominantly methoxy group) with good antimalarial activity are available in literature [19,25,26]; however the effect of *O*- and *C*-allyl groups at different positions of ring A remains to be elucidated. Accordingly, more than forty allylated chalcones were synthesized and screened for their antiplasmodial activity against *Pf*3D7 strain using a validated, micro titer plate based highthrough-put SYBR green I fluorescence technique [47].

2.2.1. C-allylated chalcones (hydroxy vs methoxy derivatives)

Initially 3-[4-hydroxy-3-methoxy-5-(prop-2-en-1-yl)phenyl]-1-(4-hydroxyphenyl)prop-2-en-1-one (**1**, Table 1) was synthesized as an analogue of Licochalcone A. However, the low activity of **1** (IC_{50}: 38.5 μM) combined with the tedious synthesis due to the presence of hydroxy substituents on both rings A and B prompted us to explore variants with enhanced activity as well as ease of synthesis. Consequently, compound **2** was synthesized by replacing the hydroxy group on ring B with the isosteric chloro group. The selection of chloro group was guided by its lipophilic nature [48] and several reports on antimalarial potency of chlorinated compounds [49–51]. Even so, no significant improvement was observed in activity (IC_{50}: 28 μM, Table 1). Moreover, the presence of hydroxy group on ring A was still proving a holdup for facile synthesis of molecules. Thus, protection of this hydroxy group was needed to proceed with the synthesis. Consequently, methylation was carried out and thus obtained compound **3** was assessed for antiplasmodial potency (Table 1). To our delight, the activity of **3** increased by almost nine fold (IC_{50}: 3.9 μM). Thereafter, keeping the substituents on ring A constant, we ventured to evaluate the effect of electron withdrawing and electron donating groups on ring B. However, all the other substitutions provided compounds with lower activity as compared to **3** indicating the importance of chloro group on ring B (**4**–**7**, Table 1).

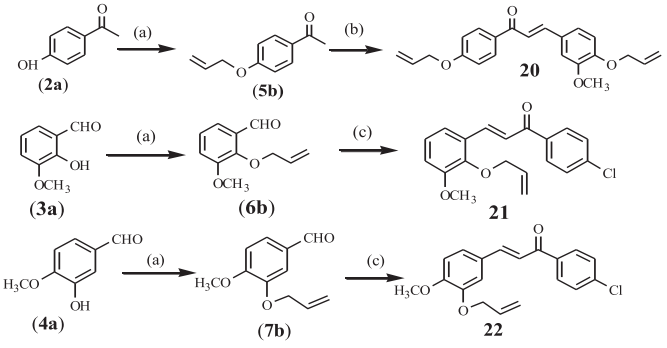

Scheme 2. Synthesis of *O*-allylated chalcones **20**–**22**. Reagents and conditions: (a) allyl bromide, potassium carbonate, anhydrous acetone, reflux; (b) 10% aq. NaOH, ethanol, **1b**, stir at rt; (c) 10% aq. NaOH, methanol, 4-chloroacetophenone, stir at rt.

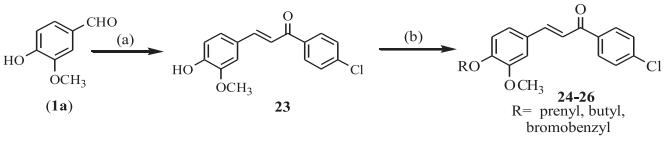

Scheme 3. Synthesis of prenylated, butylated and 4-bromobenzylated chalcones (**23**–**26**). Reagents and conditions: (a) KOH, ethanol, 4-chloroacetophenone, stir at rt; (b) prenyl bromide or 1-bromobutane or 4-bromobenzyl bromide, potassium carbonate, anhydrous acetone, reflux.

2.2.2. C- and O-allylated chalcones (effect of allyloxy group)

To make the initial template more lipophilic, allyloxy group (**8**) was introduced [40] in place of hydroxyl position of **2**. It resulted in slight decrease of activity (IC_{50}: 7.8 μM) when compared with **3** (IC_{50}: 3.9 μM) though it was still considerably higher than **2** (IC_{50}: 28 μM) (**8** *vs* **3** *vs* **2**, Table 1).

2.2.3. O-allylated chalcones and structure–activity investigations

To appraise the effect of removal of *C*-allyl group, compound **9** was prepared and evaluated against *Pf*3D7. Delightedly, **9** with IC_{50}: 2.5 μM (Table 2) turned out to be more potent than both Licochalcone A (IC_{50}: 4.1 μM) and its well-reported analogue [23], 4-dimethoxy-4′-butoxychalcone (IC_{50}: 8.9 μM). Thereafter, the structure–activity studies were carried out by varying the substitutions on ring B (**10**–**20**, Table 2). It is clear that introduction of 3,4-dichloro (**10**), bromo (**11**), iodo (**12**), fluoro (**13**), 3-chloro (**14**), methoxy (**15**), methylenedioxy (**16**), nitro (**17**), amino (**18**) or allyl (**20**) group (Table 2) did not lead to enhancement of activity when compared to chalcone **9**.

We next ventured to evaluate the positional importance of allyl group (*ortho vs meta vs para*) on ring A. The fact that activity was markedly affected by changing the position of allyl group at the phenyl ring (**21** & **22** *vs* **9**, Table 3) emphasized the importance of para-substitution of *O*-allyl group for activity. Subsequently, the effect of changing the nature of the *O*-substituent (H, prenyl, C_4H_9 and $CH_2C_6H_4Br$) was evaluated and reduced activity was observed

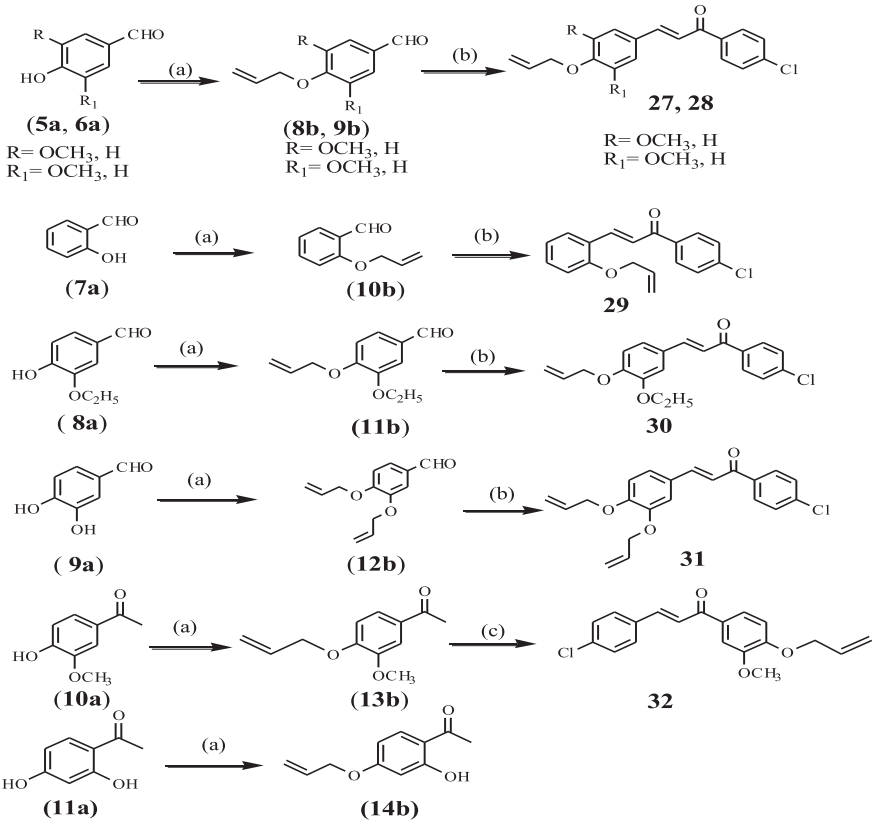

Scheme 4. Synthesis of *O*-allylated chalcones (**27**–**32**) containing vanillin and its analogues. Reagents and conditions: (a) allyl bromide, potassium carbonate, anhydrous acetone, reflux; (b) 10% aq. NaOH, ethanol, 4-chloroacetophenone, stir at rt; (c) 10% aq. NaOH, ethanol, 4-chlorobenzaldehyde, stir at rt.

in each instance (**23**–**26**, Table 3). Likewise, any change in the position, nature and number of methoxy groups at ring A markedly affected the activity (**27**–**31**, Table 3), signifying the particularly special contribution of 3-methoxy group (as revealed in compound **9**), which might be due to its orientation and binding ability with the target protein(s) of the malaria parasite.

In the backdrop of a study by Liu et al. [52], where size parameter of ring B (large, alkoxylated) and electron deficient

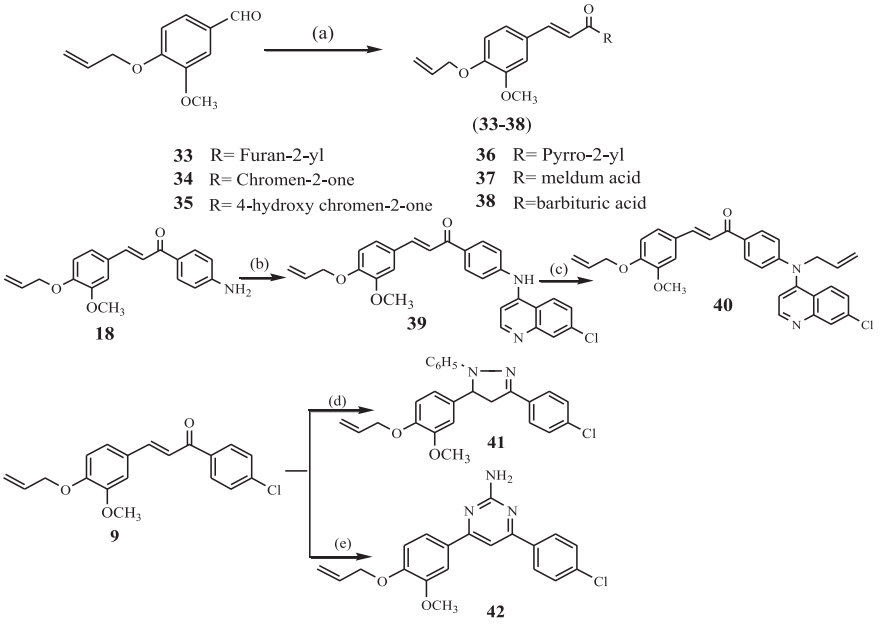

Scheme 5. Synthesis of allylated chalcones (**33**–**42**) containing heteroaromatic moiety. Reagents and conditions: (a) aq. NaOH, ethanol, substituted heteroatomic acetophenone stir, rt; (b) 4,7-dichloroquinoline; THF, reflux; (c) allyl bromide, KOH, THF, CTAB, stir rt; (d) phenylhydrazine, sodium acetate, aq. acetic acid, MW at $P = 180$ W for 30 min; (e) guanidine HCl, KOH, ethanol, reflux.

Table 1
Antiplasmodial activity, resistance and therapeutic indices of *C*- and both *C*- & *O*-allylated chalcones.

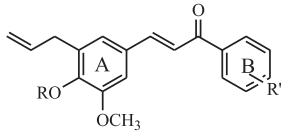

1. R =H, R'= 4-OH
2. R= H, R'= 4-Cl
3. R= CH_3, R'= 4-Cl
4. R= CH_3, R'= 4-OCH_3
5. R= CH_3, R'= 3,4-OCH_2O-
6. R= CH_3, R'= 4-Br
7. R= CH_3, R'= 4-NO_2
8. R= allyl, R'= 4-Cl

Compd. no.	Mol. Wt	IC_{50} (μM) *Pf*3D7	IC_{50} (μg/mL) *Pf*3D7	Resistance index		Therapeutic index	
				IC_{50} Indo/IC_{50} 3D7	IC_{50} Dd2/IC_{50} 3D7	IC_{50} HeLa/IC_{50} 3D7	IC_{50} L929/IC_{50} 3D7
1	310.3	38.5	11.9	0.6	0.6	1.5	1.4
2	328.7	28	9.21	1.9	1.5	>3.6	3.3
3	342.8	3.9	1.34	3.6	1.2	6.9	7.4
4	338.4	4.3	1.45	3.5	0.9	12.8	12.8
5	352.3	4.7	1.65	2.0	1.2	8.5	6.4
6	387.2	5.3	2.05	2.9	0.8	3.0	10
7	353.3	12.5	4.41	>4	2.2	7.8	4.6
8	368.8	7.8	2.87	>2.6	1.0	8.3	1.9
CQ	319.9	40 nM	0.012	11	4.2	>200	>200

nature of ring A were found significant for antiplasmodial activity, **32** was synthesized by swapping of substituents between rings A and B of **9**. However, **32** exhibited lesser antiplasmodial potential (IC_{50}: 8.6 μM, Table 3) as compared to **9** (Table 2), thus underlying the importance of enhanced electron density on ring A of chalcone for good activity [53].

2.2.4. Effect of incorporation of heterocyclic moiety

Heteroaryl substitution is an attractive strategy for the development of drugs with desirable activity and several inspiring reports on the antiplasmodial activity of heterocyclic chalcone derivatives [54] provided us the impetus to synthesize such analogues. To begin with, we designed chalcones by the condensation of **1b** with different heterocyclic carbonyls like 2-acetylfuran (**33**), 3-acetylcoumarin (**34**), 3-acetyl-4-hydroxycoumarin (**35**) [55], 2-acetylpyrrole (**36**), meldrum acid (**37**) and barbituric acid (**38**). However, in each case the antiplasmodial potential was found to be significantly reduced (**33**–**38**, Table 4). Given that quinoline, particularly with 7-chloro group, is considered an excellent lead prototype for the development of antiplasmodial drugs [56,57] compound **39** was synthesized which, however, was found to be quite inactive against malarial parasites. Interestingly, *N*-allylation of **39** significantly improved the activity of resulting compound (**40** *vs* **39**, Table 4). In a similar vein, cyclization of chalcones leading to the synthesis of heterocycles, such as pyrazoles and pyrimidines, is of great interest in drug designing because of their broad spectrum of biological activities [45,58]. However, in our case, introduction of pyrazole ring at double bond (**41**) had little or no effect on activity while pyrimidine derivative (**42**) displayed considerable loss of activity (Table 4).

2.2.5. Resistance and therapeutic indices

The identified lead chalcones were also tested against chloroquine resistant strains of *P. falciparum* (Dd2 and INDO) (Tables 1–4). Against a resistance Index (IC_{50} Dd2/IC_{50} 3D7) of 4.2 for chloroquine, the indices for the potent chalcones were found to be in the range of 0.5–5.9 (Tables 1–4). Finally, the active compounds were analyzed for their cytotoxic behavior against two mammalian cell

Table 2
Antiplasmodial activity, resistance and selectivity indices of *O*-allylated chalcones.

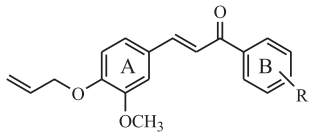

	R		R		R
9	4-Cl	**13**	4-F	**17**	4-NO_2
10	3,4-diCl	**14**	3-Cl	**18**	4-NH_2
11	4-Br	**15**	4-OCH_3	**19**	H
12	4-I	**16**	3,4-OCH_2O-	**20**	4-O-allyl

Compd. no.	Mol. Wt	IC_{50} (μM) *Pf*3D7	IC_{50} (μg/mL) *Pf*3D7	Resistance index		Therapeutic index	
				IC_{50} Indo/IC_{50} 3D7	IC_{50} Dd2/IC_{50} 3D7	IC_{50} HeLa/IC_{50} 3D7	IC_{50} L929/IC_{50} 3D7
9	328.8	2.5	0.82	6.6	1.2	20.8	23.2
10	363.2	10	3.63	>2	0.5	>10	8.7
11	373.2	8.1	3.02	>2.5	0.9	20.5	>12.5
12	420.2	8.5	3.57	>2.4	0.8	13	11.8
13	312.3	23	7.78	0.7	0.8	1.8	2.1
14	328.8	5.3	1.74	2.6	0.7	2.5	9.4
15	324.4	22.5	7.29	0.6	1.3	0.8	2.9
16	338.4	38.5	13.05	0.6	1.1	>2.6	2.2
17	339.3	>50	>16.9	nd	nd	nd	nd
18	309.4	36	11.13	0.4	0.6	1.8	1.4
19	294.3	38	11.18	0.4	0.7	1.2	2.6
20	350.4	7.4	2.59	1.6	0.5	4.9	9.7
CQ	319.9	40 nM	0.012	11	4.2	>200	>200

nd = not tested.

Table 3
SAR investigation for antiplasmodial activity, resistance and selectivity indices.

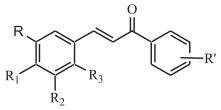

21 R=R_1= H, R_2= OCH_3, R_3= *O*-allyl, R'= 4-Cl
22 R=H, R_1= OCH_3, R_2= *O*-allyl, R_3= H, R'= 4-Cl
23 R=H, R_1= OH, R_2= OCH_3, R_3= H, R'= 4-Cl
24 R=H, R_1= *O*-prenyl, R_2= OCH_3, R_3= H, R'= 4-Cl
25 R=H, R_1= *O*-butyl, R_2= OCH_3, R_3= H, R'= 4-Cl
26 R=H, R_1= *O*-$CH_2C_6H_4Br$, R_2= OCH_3, R_3= H, R'= 4-Cl
27 R=OCH_3, R_1= *O*-allyl, R_2= OCH_3, R_3= H, R'= 4-Cl
28 R=H, R_1= *O*-allyl, R_2=R_3= H, R'= 4-Cl
29 R=R_1=R_2=H, R_3= *O*-allyl, R'= 4-Cl
30 R=H, R_1= *O*-allyl, R_2= OC_2H_5, R_3= H, R'= 4-Cl
31 R=H, R_1= R_2=*O*-allyl, R_3= H, R'= 4-Cl
32 R=H, R_1=Cl, R_2=R_3= H, R'= 3-*O*-allyl, 4-OCH_3

Compd. no.	Mol. Wt	IC_{50} (μM) *Pf*3D7	IC_{50} (μg/mL) *Pf*3D7	Resistance index		Therapeutic index	
				IC_{50} Indo/IC_{50} 3D7	IC_{50} Dd2/IC_{50} 3D7	IC_{50} HeLa/IC_{50} 3D7	IC_{50} L929/IC_{50} 3D7
21	328.8	12.5	4.11	>1.6	0.8	1.0	3.8
22	328.8	18	5.92	1.05	0.94	2.3	4.2
23	288.7	28	8.09	1.2	1.3	1.1	2.4
24	356.8	5.0	1.78	4.6	0.9	5.2	5.4
25	344.8	14.8	5.0	1.22	0.84	>6.8	>6.8
26	457.7	8.0	3.84	3.71	2.6	>12	>12
27	358.8	3.8	1.36	4.5	5.9	7.9	11.6
28	298.8	43	12.84	0.74	0.72	2.3	1.5
29	298.8	9.0	2.69	2.2	1.0	>11.1	5.6
30	342.8	28	9.60	0.64	0.75	1.8	2.5
31	354.8	3.4	1.21	4.9	1.0	6.8	29.4
32	328.8	8.6	2.83	>2.3	1.3	4.1	6.0
CQ	319.9	40 nM	0.012	11	4.2	>200	>200

lines *viz*. HeLa and fibroblast L929. The obtained therapeutic indices (IC_{50} HeLa cell line/IC_{50}*Pf*3D7) values indicated that the most active compounds (**9**, **40**, **41**) were also relatively non-toxic.

2.2.6. *Antiplasmodial activity of combinations of **9** with **CQ** and **ART***

In vitro antiplasmodial studies using combinations of **CQ**/**ART** and **9** (Table S1, see SI) were performed by SYBR Green I assay on ring stage synchronized cultures of *Pf*3D7 and *Pf*INDO. As shown in isobolograms (Fig. 1) the combinations of **CQ** and **9** (Tables S2 and S3 see SI) showed weak synergy (ΣFIC$_{50}$: 0.69) to additivity (ΣFIC$_{50}$: 1.17–1.94) to mild antagonism (ΣFIC$_{50}$: 2.16) against *Pf*INDO (Fig. 1; A1) while the same combination showed additivity (ΣFIC$_{50}$: 1.45–1.77) to mild antagonism (ΣFIC$_{50}$: 2.60–2.83) against *Pf*3D7 (Fig. 1; B1). In contrast, combination of **ART** and **9** (Tables S4 and S5 see SI) in the molar ratio 1:500 exhibited strong synergy (ΣFIC$_{50}$: 0.31) against *Pf*INDO (Fig. 1; A2). Other ratios of this combination showed moderate to weak synergy (ΣFIC$_{50}$: 0.42–0.72). In the synergy

Table 4
Antiplasmodial activity, resistance and selectivity indices of heterocyclic derivatives of *O*-allylated chalcones.

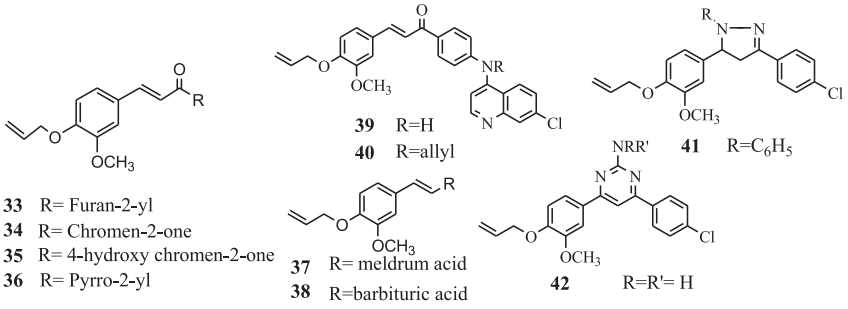

33 R= Furan-2-yl
34 R= Chromen-2-one
35 R= 4-hydroxy chromen-2-one
36 R= Pyrro-2-yl
37 R= meldrum acid
38 R=barbituric acid
39 R=H
40 R=allyl
41 R=C_6H_5
42 R=R'= H

Compd. no.	Mol. Wt	IC_{50} (μM) *Pf*3D7	IC_{50} (μg/mL) *Pf*3D7	Resistance index		Therapeutic index	
				IC_{50} Indo/IC_{50} 3D7	IC_{50} Dd2/IC_{50} 3D7	IC_{50} HeLa/IC_{50} 3D7	IC_{50} L929/IC_{50} 3D7
33	284.3	95	26.9	nd	nd	nd	nd
34	362.4	100	36.2	nd	nd	nd	nd
35	378.3	>100	>37.8	nd	nd	nd	nd
36	283.3	48	13.58	1.3	0.7	>2.1	>2.1
37	318.3	>100	>31.8	nd	nd	nd	nd
38	302.3	>100	>30.2	nd	nd	nd	nd
39	470.9	75	35.33	nd	nd	nd	nd
40	511.0	3.5	1.79	1.9	0.9	10.6	16.9
41	418.9	3.3	1.38	5.2	0.9	>60.6	>60.6
42	367.8	>50	>18.4	nd	nd	nd	nd
CQ	319.9	40 nM	0.012	11	4.2	>200	>200

nd = not tested.

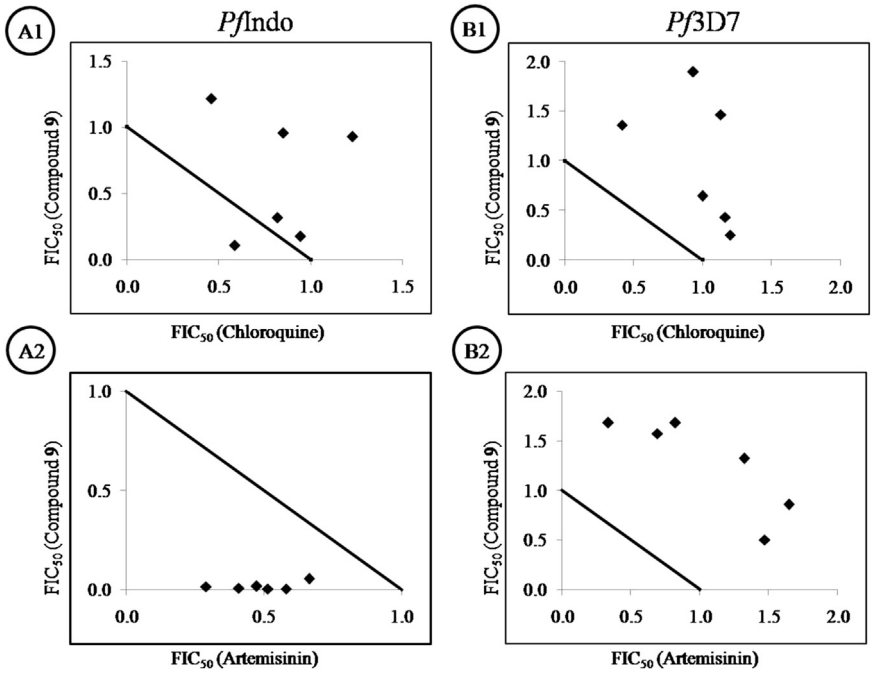

Fig. 1. Isobolograms showing combination effects between Artemisinin (**ART**)/Chloroquine (**CQ**) and **9** against CQ resistant *Pf*INDO (left panel) and CQ sensitive P*f*3D7 (right panel). Note the marked synergy effects between **ART** and **9** against P*f*INDO (A2).

combinations, the IC_{50}s of **9** and **ART** were reduced 16 to 320 times and 1.3 to 3.2 times, respectively (Table S2, see SI). However, the same combinations displayed additivity (ΣFIC_{50}: 1.97–2.01) to mild antagonism (ΣFIC_{50}: 2.27–2.64) against *Pf*3D7 (Fig. 1; B2).

2.2.7. Stage specific study of cytostatic vs cytocidal actions of individual drugs and drug combinations

In order to find if drug treatments were cytostatic or cytocidal, we first exposed ring stage synchronized *Pf*INDO cultures to individual drugs or combinations of drugs at their respective IC_{100} for stage dependent specified times (rings: 6, 24, 48 h; trophozoites: 18, 24 h, schizonts: 12 h). Thereafter, the cultures were washed free of drugs using RPMI and allowed to grow in drug free media for specified times. Results of SYBR green I assay (Fig. 2A) revealed that standard antimalarial drugs *viz*. **CQ** and **ART** were cytocidal against ring stage parasite. However, while **CQ** was found to be cytocidal at 6 h, **ART** exhibited its cytocidal action much later at 24 h. Against trophozoites, both **CQ** and **ART** were found to have cytocidal action upon exposure for 24 h. The ring and trophozoite results described above were fully confirmed by microscopic analysis of Giemsa stained smears (Fig. 2B, for zoom of Fig. 2B see Figs. S1 and S2). Both **CQ** and **ART** allowed the transition of schizonts to rings. However while the rings emanating from **CQ** treated cultures failed to grow and were not seen in smears made after 48 h of incubation in drug free medium, the rings in **ART** treated cultures were found to complete a full ring to ring cycle in 48 h as evidenced by increased parasitemia. The unique features of rings emanating from **ART** *vs* **CQ** treated cultures were evident also in the results of the SYBR Green assay which showed high parasitemia in the former than in the latter case (Fig. 2A). This observation seems to have striking *in vitro* resemblance to the delayed parasite clearance time that is being clinically observed in patients undergoing ACT.

It has been suggested that artemisinin stressed parasites have the ability to enter into a non dividing state of dormancy from which they tend to revive into proliferation once the drug pressure is reduced [59]. In contrast to **CQ** or **ART**, **9** was found to inhibit *P. falciparum* at all stages of the life cycle including ring, trophozoite and schizont stages. Further drug withdrawal followed by culture in drug free medium confirmed that **9** was cytocidal since the parasites failed to revive during drug free incubations (Fig. 2). The SYBR Green I assay showed that **9** caused complete inhibition of growth of ring, trophozoite and schizont stages at 24 h, 18 h and 12 h of drug exposure, respectively. It may be noted that **9** caused substantial inhibition of growth (~40%) of ring stage culture as observed at 6 h (Fig. 2A) indicating that it may be fast in acting against the ring stage. It is worth mentioning that rapid action against early ring stages is a cherished virtue for an antimalarial since it can curtail the rise of parasitemia much before replication sets in. The effect of drug combinations at synergy concentrations (ΣFIC_{100}: 0.69 for **CQ** + **9**; ΣFIC_{100}: 0.31, 0.49 for **ART** + **9**) against different stages of malaria parasites (Fig. 2A and B) indicated that the IC_{100} of **CQ** + **9** combination killed the parasite at ring and trophozoite stages while it allowed the growth of schizonts. In contrast, while the **ART** + **9** combinations tested at IC_{100} stalled the growth of ring and trophozoite stage parasites, they caused only partial killing of the ring and trophozoite stages. Further both combinations (ΣFIC_{100}: 0.31, 0.49) did not influence the growth of schizonts. The 2X ΣFIC_{100} of **ART** + **9** caused complete mortality of ring stage parasites, marginal mortality of trophozoites and exerted no effect on the schizonts (Fig. 2C). A model depicting the characteristic antiplasmodial traits of **ART**, **CQ** and **9** is shown in Fig. 3.

Earlier, Wang et al. have reported that **ART** inhibits the growth of *Plasmodium* by acting directly on the mitochondria of the malaria parasites [60]. The strong synergy in **ART** + **9** combination observed against *Pf*INDO may have its origins in the fact that both **ART** and **9** might have mitochondrion as the common target [61]. However, an intriguing observation was the strong synergy in the action of **ART** + **9** combination against **CQ** resistant P*f*INDO but additivity to mild antagonism from the same against the **CQ** sensitive P*f*3D7. Earlier studies have also reported additive effects or weak synergy of combinations of chalcone derivatives and ART against **CQ** sensitive P*f*3D7 [62]. The phenomenon of strong synergy in combinations of chalcone and **ART** observed against **CQ** resistant P*f*INDO for the first time in the present study may be associated

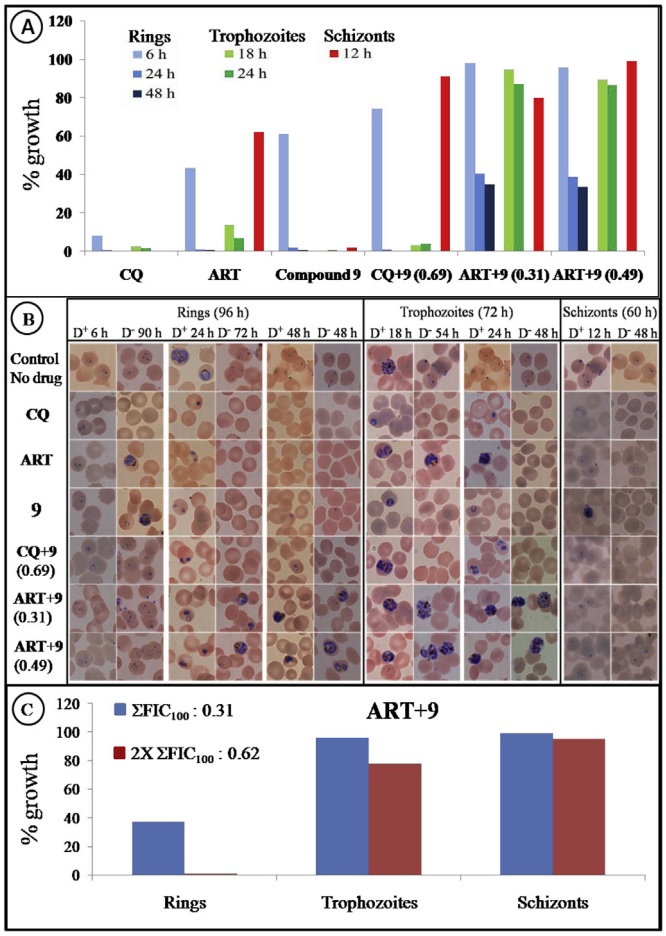

Fig. 2. Evaluation and kinetics of the action of individual drugs and drug combinations on the growth and survival of different stages of *Pf*INDO in *in vitro* culture. Synchronized ring, trophozoite and schizont *in vitro* cultures of *Pf*INDO were treated with IC_{100} of individual drugs (**9**, **CQ**, **ART**) or combinations thereof. Values in parentheses indicate ΣFIC_{100} of the combination in each case. Drug exposure times (h) were 6, 24 and 48 for rings, 18 and 24 for trophozoites and 12 for schizonts. In each case, drug was withdrawn, cells washed and reconstituted in drug free media for a total of 96 h (rings), 72 h (trophozoites) and 60 h (schizonts). (A) Evaluation of growth inhibition by SYBR Green lysis method. (B) Microscopic evaluation of Giemsa stained smears. (For zoom of Fig. 2B see Figs. S1 and S2, SI). (C) Comparative effect of 1X *vs* 2X ΣFIC_{100} of **ART** + **9** combinations on the growth of different stages of the life cycle of *Pf*INDO.

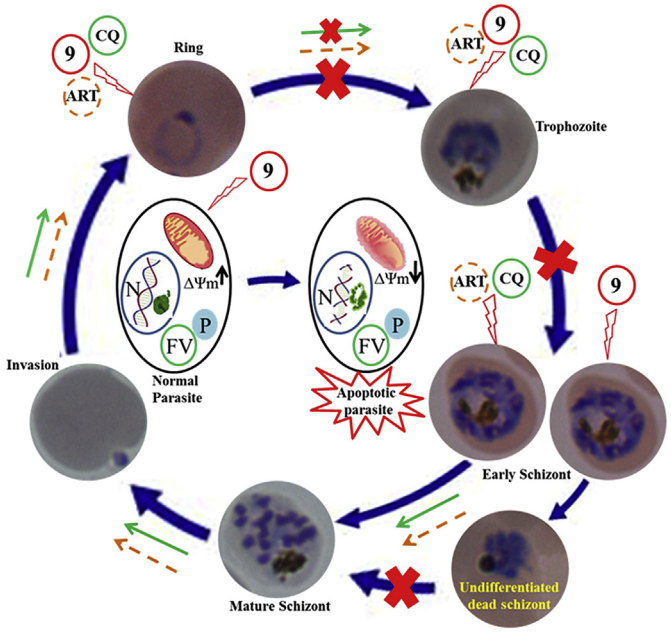

Fig. 3. Stage specificity of antiplasmodial actions of **ART**, **CQ** and **9**. Blue closed head solid arrows indicate the changing stages of the normal cell cycle of *Plasmodium falciparum*. Drugs were given to each stage in separate experiments and the results monitored by microscopic examination of Giemsa stained smears. All the three molecules taken at respective IC_{100} inhibited (red cross) the growth of ring and trophozoite stages. While **ART** (Orange dotted line open head arrows) and **CQ** (green solid line open head arrows) allowed the progression of early schizonts all the way to egress of merozoites, **9** (blue closed head solid arrows) which gave undifferentiated dead schizonts, appeared to block the process of schizont maturation reflected in absence of well arrayed pattern of merozoites, lack of egress and invasion of new red blood cells. Interestingly (as shown in Fig. 2B) in early schizonts cultured in drug free medium (D-) following treatment with **ART**/**CQ** for 12 h (D+), although well formed rings were observed in both the cases, the **CQ** treated culture failed to form trophozoites while the **ART** treated culture completed the 2nd cycle in full. Ring and trophozoite stages of the parasite life cycle on treatment with **9** showed signs of apoptotic death including loss of mitochondrial membrane potential (ΔΨm), DNA fragmentation (WWW) and chromatin condensation (●). (For interpretation of the references to color in this figure legend, the reader is referred to the web version of this article.)

with the presence of unique drug transporter proteins in **CQ** resistant strains. As indicated by earlier studies, **ART** is preferentially taken up by malaria parasite infected red blood cells and the characteristics of this uptake have suggested the likelihood of a carrier mediated partitioning of **ART** into parasitized red blood cells [62]. We suggest that **9** may modulate the activity of such an unidentified transporter to enhance the active uptake of **ART** resulting in marked synergy with IC_{50}s of **9** + **ART** combination falling by as much as 320 fold (**9**) and 3.2 fold (**ART**) (Table S4, see SI). The observation of an inverse relation between increasing concentration of **9** in the **ART** + **9** mixtures and the decreasing IC_{50} of **ART** in the same points to a chemo-sensitizing function of **9** towards uptake of **ART** (Fig. 4).

It may be noted that the linear decrease observed for the first four data points is followed by two data points that show a reversal of this trend. This mixed trend may suggest the presence of two different binding sites for **9** on the postulated carrier protein. The high affinity binding site may account for the chemo-sensitizing effect that lowers the IC_{50} of **ART** with increasing concentration of **9**. Occupancy of the low affinity binding site at higher concentrations of **9** (last two data points in Fig. 4) may lead to a conformational change in the carrier protein that is not consistent with the fully activated state of the carrier protein. This model (Fig. 5) is consistent with the fact that IC_{50} of **9** alone (16.5 μM) *vs* the lowest IC_{50} of **9** in the **ART** + **9** combinations (52 nM) (Table S4, see SI) are different by over two orders of magnitude. The growth inhibition curve of **9** alone (Fig. S3, see SI) indicates that at such low concentrations, **9** alone fails to exhibit any growth inhibition. Therefore the "killer" molecule in the **ART** + **9** combinations must be **ART** whose uptake may be activated by interactions of **9** with the postulated drug transporter protein.

2.2.8. *Induction of apoptosis in* **9** *treated P. falciparum*

We have observed the hallmark features of programmed cell death including DNA fragmentation and loss of mitochondrial membrane potential (ΔΨm) in **9** treated ring and trophozoite stages of *P. falciparum* at IC_{100} (Fig. 6). Alteration in mitochondrial membrane permeability is one of the key features of apoptotic cell death. The change in ΔΨm was detected by JC-1 (5,5′,6,6′-tetrachloro-1,1′,3,3′-tetraethylbenzimidazolylcarbocyanine iodide) probe using fluorescence microscopy. At high ΔΨm, the membrane potential sensitive JC-1 aggregates in the mitochondria and emits red-fluorescence at 590 nm while at low ΔΨm, JC-1 exists as monomers in the cytoplasm and emits green-fluorescence at 529 nm. Upon treatment with **9**, a decline in ΔΨm first observed at 6 h

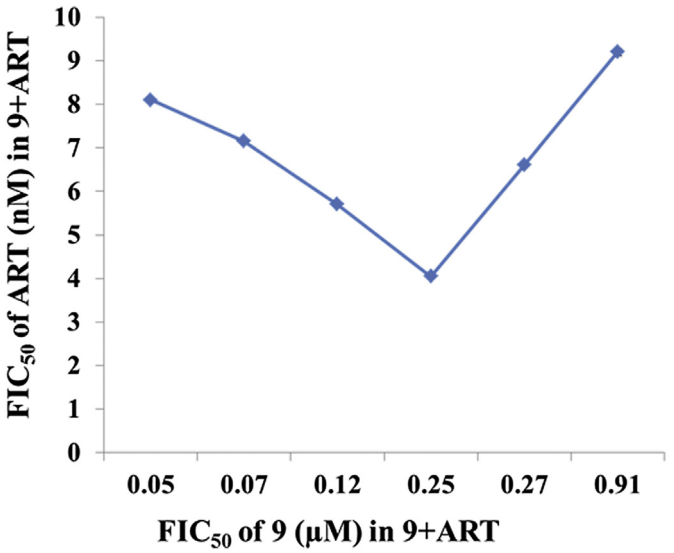

Fig. 4. Plot of varying FIC_{50} (Fractional Inhibitory Concentration 50%) of **9** and **ART** in **9** + **ART** combinations tested against **CQ** resistant *Pf*INDO. Note the inverse relation between increasing concentration of **9** and decreasing concentration of **ART** for the first four data points. The last two data points are however showing a reverse trend suggesting the presence of high and low affinity binding sites in the postulated **ART** transporters as discussed in the text.

becomes stronger at 12 h and attains a state of complete loss at 48 h. In contrast to rings, trophozoites showed complete loss of their ΔΨm at 12 h (Fig. 6). Similar loss of ΔΨm has earlier been reported upon treatment of *P. falciparum* cultures with **CQ**, *Solanum nudum* steroids and etoposide [63]. Totino et al. [64] have reported that treatment with either staurosporine or S-nitroso-*N*-acetyl-penicillamine (SNAP) resulted in loss of ΔΨm in *P. falciparum*. Fragmentation and degradation of DNA and changes in nuclear morphology are other major indicators for apoptosis. Hoechst 33342 (2′-[4-ethoxyphenyl]-5-[4-methyl-1-piperazinyl]-2,5′-bis-(1*H*) benzimidazole trihydrochloride trihydrate) stain was used to detect DNA fragmentation in *P. falciparum*. Hoechst stain is a cell permeable DNA binding fluorescent dye that emits strong blue fluorescence at 460 nm from apoptotic cells while it gives low intensity fluorescence in healthy cells. This intensity difference is a consequence of the reduced number of binding sites for the dye on the highly condensed super coiled native state of chromatin in healthy cells. In contrast, fragmented chromatin associated with apoptosis provides an increased number of binding sites resulting in bright staining of fragmented chromatin [65]. Thus, the strong staining seen at 24 h in **9** treated trophozoites suggests marked DNA fragmentation. Likewise, the increased fluorescence intensity in **9** treated ring stage parasites *vs* the faint intensity observed for untreated rings (Fig. 6) provided evidence for DNA fragmentation. Further evidence in support of an apoptotic death involving DNA degradation can be seen in the drug exposure followed by drug withdrawal experiment (Fig. 2B) where **9** treated ring, trophozoite and schizont stage parasites failed to show Giemsa positive parasites when observed at 96, 72 and 60 h, respectively. Similarly **CQ** and *S. nudum* steroids have been reported to induce DNA fragmentation in *P. falciparum* [63]. Seminal features of apoptosis have earlier been observed by us in *P. falciparum* cultures treated with stilbene-chalcone hybrids [66].

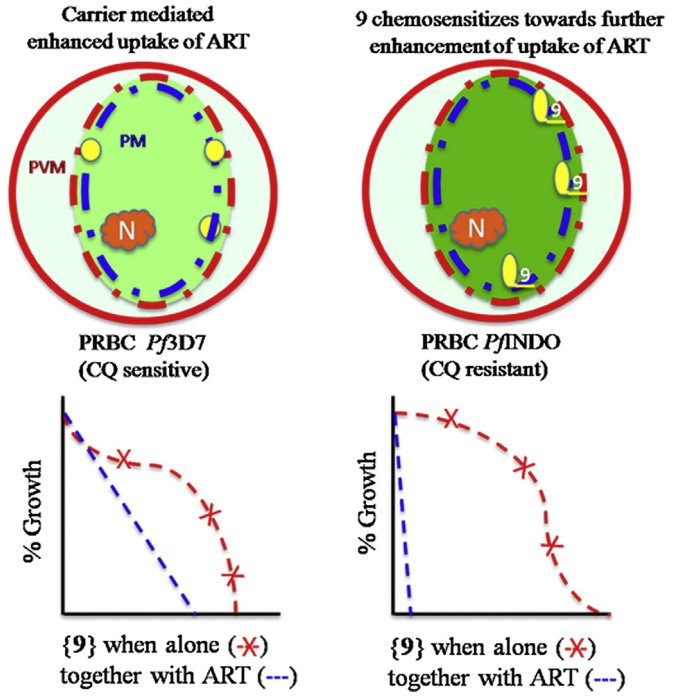

Fig. 5. Chemo-sensitizing effect of **9** in the antiplasmodial action of **ART** against **CQ** resistant PfINDO. Carrier (yellow filled small circles) mediated transport is known to cause preferential uptake (light green coloration) of **ART** by *Plasmodium* infected red cells over uninfected cells. The combination (**9** + **ART**) leads to weak synergy in the **CQ** sensitive *Pf*3D7 (left top and bottom panels). In **CQ** resistant *Pf*INDO (right panels) a mutant version of the carrier protein seems to bind **9** causing a chemo-sensitizing effect that results in further enhanced uptake of **ART** (deep green color) leading to strong synergy in the **ART** + **9** combination. (For interpretation of the references to color in this figure legend, the reader is referred to the web version of this article.)

It is interesting to find if the origins of apoptosis as seen in higher eukaryotes can be traced back to lower eukaryotes like the malaria parasite. Even as the end points of apoptosis including loss of mitochondrial membrane potential and DNA fragmentation have been observed, it is not clear if the classical apoptotic machinery exists in *Plasmodium*. In this context, the findings of Metacaspase-Like Protein (*Pf*MCA1) [67] in erythrocytic stages of *P. falciparum* and the caspase like activity in *P. berghei* ookinetes [68] seem to provide support for the existence of the classical apoptotic machinery in *Plasmodium*. It is well appreciated that all higher eukaryotic cells are endowed with pro and anti apoptotic mechanisms to enable the cell to use them “wisely”. Similar seems to be the case with *Plasmodium* where inhibition of host hepatocyte cell death during invasion of sporozoites is necessary for survival and development of liver stage parasites. Rennenberg et al. [69] have found that *P. berghei* inhibitor of cysteine proteases (PbICP) or its homolog falstatin/PfICP in *P. falciparum* play an important role in sporozoite invasion of host cells and in parasite survival during liver stage development by inhibiting proteases of the parasite and proteases of the host involved in programmed cell death. In our study, we have observed the hallmarks of apoptosis including DNA fragmentation, DNA degradation and disruption of ΔΨm in drug treated parasites while the untreated parasites failed to show the same features. Drug induced apoptosis as seen in our study could be a consequence of the drug activating the pro-apoptotic machinery or inhibiting the anti-apoptotic machinery of *Plasmodium*. The molecular difference between the proteins that constitute the apoptotic machineries of unicellular and multicellular organisms makes the apoptotic pathway a persuasive and promising target for novel antiplasmodial drugs.

2.3. Physico-chemical parameters calculation of allylated chalcones (*1*–*42*)

The molecular properties for absorption, distribution, metabolism and excretion (ADME) are crucial to enhance the probability of success through the drug development stage [70–77]. The

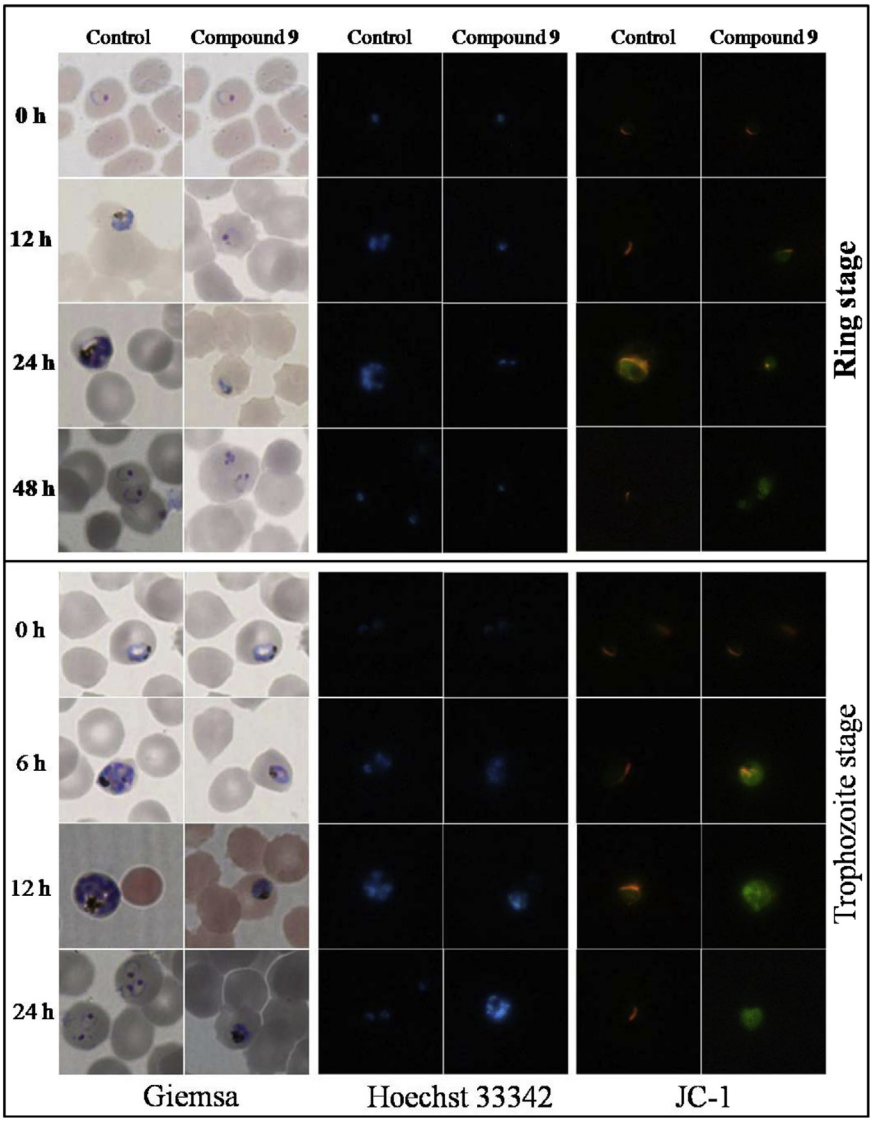

Fig. 6. Induction of apoptosis in *P. falciparum* by **9**. The synchronized ring and trophozoite stages of *P. falciparum* treated with IC_{100} of **9** for different times (indicated on the left) have been evaluated by optical (Giemsa) and fluorescence microscope {Hoechst 33342(DNA binding dye) and JC-1(mitochondrial membrane potential sensor dye)}. The key features of apoptosis including DNA fragmentation and loss of mitochondrial membrane potential ($\Delta\Psi m$) can be seen in both ring and trophozoite stage parasites.

generally low solubility of chalcones has been one of the major obstacles in the development of this type of compounds to usable drugs: The compounds do not dissolve in the intestine and are not available for absorption, making the bioavailability extremely low and the dose level unrealistically high.

Absorption is a primary focus in drug development and medicinal chemistry since the drug must be absorbed in the body before any medicinal effects can take place. This requirement makes lipophilicity and solubility the two major properties responsible for absorption and bioavailability of drugs [74,75]. The 1-octanol-water partition coefficient, log P, is a well known parameter to estimate lipophilicity (or solubility in lipids) of chemical compounds [76]. Aqueous solubility (AlogS) is usually measured as with logarithm of intrinsic or pH-dependent solubility [77]. Similarly, topological polar surface area (TPSA) is a good indicator of drug absorbance in the intestines, Caco-2 monolayers penetration, and blood–brain barrier crossing [78]. It has been well established that optimal lipophilicity range along with low molecular weight and low polar surface area is the major driving force that leads to good absorption of compounds in the intestine by passive diffusion [71] while a very high TPSA value contributes for a low bioavailability for the molecule [72].

Accordingly, a computational study for prediction of ADME properties of the allylated chalcones (**1**–**42**) was performed [79] and is presented in Table S6 (see SI). From all the parameters, it was observed that all the active chalcones exhibited a low TPSA value when compared to Licochalcone (LC) and hence greater %Abs ranging from 85.9 to 99.9%. Furthermore, all the active molecules violate none or only one of Lipinski's parameters, thus making them potentially promising agents for antimalarial therapy.

3. Conclusion

The present SAR study of chalcones suggests that the allyl (*O*-allyl or *C*-allyl or both) and methoxy substituents on ring A and presence of chloro or methoxy group on ring B (as in **3**, **4**, **9**, **27**, **31**), an *N*-allylated quinoline substitution on ring B (as in **40**) or pyrazole substituent on α, β unsaturated core (as in **41**) are required for good antiplasmodial activity of chalcones. Further, the drug combination studies of the most potent compound **9** revealed that the

combination of **9** with **ART** displayed strong synergy (the IC_{50} of **9** and **ART** were reduced by 320 and 3 fold, respectively) while the combination of **9** with **CQ** displayed weak synergy in the **CQ** resistant P*f*INDO strain. Interestingly, **9** showed cytocidal effects on all three erythrocytic stages (ring, trophozoite and schizont) of malaria parasite. Also, the chromatin alterations and disruption of $\Delta\Psi m$ revealed the possibilities of programmed cell death in *P. falciparum* which was in turn confirmed by the morphological changes and time dependent disappearance of DNA content in Giemsa stained parasites. Optimum drug like properties as determined by physico-chemical investigations and low cytotoxic values of these compounds suggest the possibility of modifying the lead candidates into clinically useful antimalarial compounds.

4. Experimental

4.1. General

All the starting materials were of reagent grade and purchased from Merck or Acros. The solvents used were obtained from Merck and used without further purification. Column chromatography was performed using silica gel (Merck, 60–120 mesh size). The chromatographic solvents are mentioned as v/v ratios. All the synthesized compounds were fully characterized by ^1H and ^{13}C NMR (Bruker Avance-300). The melting points were determined on a digital Barnsted Electrothermal 9100 apparatus. HRMS-ESI spectra were determined using micromass Q-TOF Ultima spectrometer and reported as *m/z* (relative intensity). FT-IR spectra were determined using Thermo Scientific Nicolet-6700 instrument. The purity of the test compounds was determined by HPLC analysis using a Shimadzu LC-20 instrument equipped with a photodiode array detector (CBM 20A) and a Purospher-Star RP-18e column (4.6 mm × 150 mm, 5 μm, Merck). Methanol-acetonitrile (70:30, v/v) (solvent A) and TFA (0.05%) (solvent B) were used as mobile phases. The above analysis indicated purity of ≥95%.

4.2. Procedure for the synthesis of chalcones

4.2.1. Procedure for the synthesis of chalcones ***1***, ***2*** *via* ***1b*** *and* ***2b*** *(Table 1, Scheme 1)*

To a 250 mL round bottom flask containing vanillin (**1a**) (1.9 mmol) in dry acetone (20 mL), allyl bromide (2.0 mmol), and anhydrous K_2CO_3 (3.8 mmol) were added. The mixture was refluxed for 6 h. After consumption of aldehyde (monitored by TLC), the mixture was filtered to remove K_2CO_3. The filtrate was vacuum evaporated and washed with hexane to remove excess of allyl bromide. The crude product was purified by silica gel column chromatography using hexane-ethyl acetate (9:1) to provide **1b**. In the second step, **1b** was taken in round bottom flask and subjected to microwave at 150 W for 15 min at 195–205 °C to undergo Claisen rearrangement. The progress of reaction was monitor with the help of TLC. The crude product was purified by silica gel column chromatography using hexane-ethyl acetate (9:1) to provide **2b**. Thereafter, to a solution of **2b** (3 mmol) and 4-hydroxyacetophenone or 4-chloroacetophenone (3 mmol) in methanol (20 mL), 10% aqueous NaOH (4 mmol) was added. The reaction mixture was stirred till completion of starting material (monitored by TLC). The reaction mixture was vacuum evaporated to remove the organic solvent and poured in cold water. The obtained precipitates were washed with dilute HCl, excess of water and methanol. The obtained residue was purified by column chromatography (silica gel, hexane: ethyl acetate (7:3; v/v)) to obtain pure chalcones (**1** or **2**) whose structure were confirmed by NMR and mass spectroscopy.

*4.2.1.1. (2E)-3-[4-Hydroxy-3-methoxy-5-(prop-2-en-1-yl)phenyl]-1-(4-hydroxyphenyl)prop-2-en-1-one (**1**).* Yellow viscous liquid (Yield 40%); ^1H NMR ($CDCl_3$, 300 MHz): δ 8.00 (2H, d, *J* = 8.64 Hz), 7.80 (1H, d, *J* = 15.54 Hz), 7.45 (1H, d, *J* = 15.54 Hz), 7.20 (2H, m), 7.01 (2H, d, *J* = 8.64 Hz), 6.87 (2H, d, *J* = 7.1 Hz), 6.12–6.01 (1H, m), 5.45 (2H, dd, *J* = 17.23, 10.50 Hz), 4.66 (2H, d, *J* = 5.39 Hz), 3.93 (3H, s); ^{13}C NMR ($CDCl_3$, 75.4 MHz): δ 190.4, 161.8, 150.8, 149.9, 145.3, 133.6, 133.0, 131.7, 130.8, 128.5, 123.5, 120.2, 118.9, 116.2, 113.4, 70.2 and 56.4. HRMS-ESI: *m/z* $[M + H]^+$ for $C_{19}H_{18}O_4$, calculated 311.1458; observed 311.1442.

*4.2.1.2. (2E)-1-(4-Chlorophenyl)-3-[4-hydroxy-3-methoxy-5-(prop-2-en-1-yl)phenyl]prop-2-en-1-one (**2**).* Yellow viscous liquid (Yield 58%); ^1H NMR ($CDCl_3$, 300 MHz): δ 7.92 (2H, d, *J* = 8.50 Hz), 7.89 (1H, d, *J* = 15.30 Hz), 7.67 (1H, d, *J* = 15.30 Hz), 7.39–7.26 (3H, m), 7.06 (2H, d, *J* = 8.50 Hz), 6.01–5.92 (1H, m), 5.10 (2H, dd, *J* = 17.22, 10.30 Hz), 4.07 (3H, s), 3.41 (2H, d, *J* = 6.76 Hz); ^{13}C NMR ($CDCl_3$, 75.4 MHz): δ 191.6, 149.9, 147.4, 146.5, 135.9, 130.2, 129.4, 128.3, 126.8, 124.7, 119.4, 116.7, 116.4, 108.7, 107.6, 56.6 and 34.1.HRMS-ESI: *m/z* $[M + H]^+$ for $C_{19}H_{17}ClO_3$, calculated 329.5913; observed 329.5927.

4.2.2. Procedure for the synthesis of chalcones ***3***–***7*** *via* ***3b*** *(Table 1, Scheme 1)*

To the **2b** (6.6 mmol) taken in round bottom flask was added sodium hydroxide (6.6 mmol) dissolved in 2 mL of water (to increase solubility benzyltrimethylammonium chloride (PTC) was added in a catalytic amount). The reaction mixture was stirred for 5–10 min. Thereafter, dimethyl sulfate (12.2 mmol) was added drop-wise to the above reaction mixture at 0 °C and then stirred at room temperature for 5–6 h. After the completion of reaction (monitored by TLC), reaction mixture was acidified with dilute HCl (pH 6) and partitioned between ethyl acetate (70 mL) and water (15 mL). The ethyl acetate layer was washed with water till neutral, dried over sodium sulfate and evaporated. The obtained residue was purified by column chromatography (silica gel, hexane: ethyl acetate (7:3; v/v)) to afford **3b**. For the synthesis of chalcones **3**–**7**, similar procedure was followed as described above.

*4.2.2.1. (2E)-1-(4-Chlorophenyl)-3-[3,4-dimethoxy-5-(prop-2-en-1-yl)phenyl]prop-2-en-1-one (**3**).* Yellow solid (Yield 72%); m.p. 65–69 °C; FT-IR (KBr, cm^{-1}) 1667; ^1H NMR ($CDCl_3$, 300 MHz): δ 7.97 (2H, d, *J* = 7.70 Hz), 7.77 (1H, d, *J* = 15.57 Hz), 7.48 (2H, d, *J* = 7.70 Hz), 7.33 (1H, d, *J* = 15.57 Hz), 7.10 (1H, s), 7.06 (1H, s), 6.03–5.94 (1H, m), 5.12 (2H, d, *J* = 11.77 Hz), 3.92 (3H, s), 3.87 (3H, s), 3.45 (2H, d, *J* = 6.39 Hz); ^{13}C NMR ($CDCl_3$, 75.4 MHz): δ 191.6, 153.4, 150.1, 145.8, 139.4, 137.1, 134.8, 130.8, 130.3, 130.1, 129.3, 123.7, 121.0, 116.5, 110.7, 61.2, 56.3 and 34.5. HRMS-ESI: *m/z* $[M + H]^+$ for $C_{20}H_{19}ClO_3$, calculated 343.6069; observed 343.6044.

*4.2.2.2. (2E)-3-[3,4-Dimethoxy-5-(prop-2-en-1-yl)phenyl]-1-(4-methoxyphenyl)prop-2-en-1-one (**4**).* Yellow solid (Yield 70%); m.p. 64–66 °C; ^1H NMR ($CDCl_3$, 300 MHz): δ 7.88 (2H, d, *J* = 6.19 Hz), 7.57 (1H, d, *J* = 15.56 Hz), 7.27 (1H, d, *J* = 15.56 Hz), 6.93 (1H, s), 6.88 (1H, s), 6.82 (2H, d, *J* = 6.27 Hz), 5.84–5.78 (1H, m), 4.94 (2H, d, *J* = 12.67 Hz), 3.75 (3H, s), 3.64 (6H, s), 3.27 (2H, d, *J* = 6.27 Hz); ^{13}C NMR ($CDCl_3$, 75.4 MHz): δ 189.4, 163.9, 153.5, 149.9, 144.6, 137.4, 134.9, 131.8, 131.3, 123.8, 123.6, 121.6, 116.6, 114.4, 110.8, 61.3, 56.4, 56.0 and 34.6. HRMS-ESI: *m/z* $[M + H]^+$ for $C_{21}H_{22}O_4$, calculated 339.1770; observed 339.1738.

*4.2.2.3. (2E)-1-(1,3-Benzodioxol-5-yl)-3-[3,4-dimethoxy-5-(prop-2-en-1-yl)phenyl]prop-2-en-1-one (**5**).* Pale yellow solid (Yield 71%); m.p. 88–92 °C; ^1H NMR ($CDCl_3$, 300 MHz): δ 7.88 (2H, d, *J* = 6.19 Hz), 7.54 (1H, s), 7.45 (1H, d, *J* = 15.56 Hz), 7.11 (2H, d,

J = 6.20 Hz), 6.90 (1H, s), 6.08 (2H, s), 6.06–5.94 (1H, m), 5.13 (2H, d, J = 14.64 Hz), 3.93 (3H, s), 3.45 (3H, s), 3.46 (2H, d, J = 5.72 Hz); ^{13}C NMR ($CDCl_3$, 75.4 MHz): δ 188.7, 153.4, 151.9, 149.7, 148.7, 144.7, 137.2, 134.7, 133.5, 131.1, 125.0, 123.4, 121.2, 116.4, 110.6, 108.9, 108.3, 102.2, 61.2, 56.3 and 34.5. HRMS-ESI: m/z $[M + H]^+$ for $C_{21}H_{20}O_5$, calculated 353.1608; observed 353.1631.

*4.2.2.4. (2E)-1-(4-Bromophenyl)-3-[3,4-dimethoxy-5-(prop-2-en-1-yl)phenyl]prop-2-en-1-one (**6**).* Yellow solid (Yield 70%); m.p. 58–60 °C; FT-IR (KBr, cm^{-1}) 1665; ^{1}H NMR ($CDCl_3$, 300 MHz): δ 7.90 (2H, d, J = 8.29 Hz), 7.77 (1H, d, J = 15.61 Hz), 7.67 (2H, d, J = 8.29 Hz), 7.38 (1H, d, J = 15.61 Hz), 7.11 (1H, s), 7.06 (1H, s), 6.04–5.95 (1H, m), 5.13 (2H, d, J = 11.40 Hz), 3.94 (3H, s), 3.93 (3H, s), 3.46 (2H, d, J = 6.38 Hz); ^{13}C NMR ($CDCl_3$, 75.4 MHz): δ 191.9, 153.5, 150.1, 146.0, 136.8, 136.7, 134.9, 132.4, 130.8, 130.5, 128.7, 123.8, 120.9, 116.6, 110.6, 61.3, 56.3 and 34.3. HRMS-ESI: m/z $[M + H]^+$ for $C_{20}H_{19}BrO_3$, calculated 388.0582; observed 388.0597.

*4.2.2.5. (2E)-3-[3,4-Dimethoxy-5-(prop-2-en-1-yl)phenyl]-1-(4-nitrophenyl)prop-2-en-1-one (**7**).* Bright yellow solid (Yield 68%); m.p. 93–96 °C; ^{1}H NMR ($CDCl_3$, 300 MHz): δ 8.38 (2H, d, J = 8.20 Hz), 8.16 (2H, d, J = 8.20 Hz), 7.80 (1H, d, J = 15.62 Hz), 7.39 (1H, d, J = 15.62 Hz), 7.13 (1H, s), 7.08 (1H, s), 6.03–5.92 (1H, m), 5.13 (2H, d, J = 11.69 Hz), 3.94 (3H, s), 3.89 (3H, s), 3.46 (2H, d, J = 6.13 Hz); ^{13}C NMR ($CDCl_3$, 75.4 MHz): δ 189.6, 153.5, 150.4, 150.3, 147.4, 143.7, 136.9, 134.9, 130.3, 130.2, 129.8, 124.2, 124.0, 120.8, 116.7, 61.3, 56.3 and 34.5. HRMS-ESI: m/z $[M + H]^+$ for $C_{20}H_{19}NO_5$, calculated 354.1561; observed 354.1579.

*4.2.3. Procedure for the synthesis of chalcone **8** via **4b** (Table 1, Scheme 1)*

To a 250-mL round bottom flask containing **2b** (1.9 mmol) in dry acetone (20 mL), allyl bromide (2.0 mmol) and anhydrous K_2CO_3 (3.8 mmol) were added. The remaining procedure was similar as described for **1b**. **4b** was obtained after column chromatography over silica gel with hexane-ethyl acetate (9:1). Chalcone **8** was synthesized using **4b** (3 mmol) and 4-chloroacetophenone (3 mmol) in methanol (20 mL), as described above which was characterized by ^{1}H & ^{13}C NMR and HRMS data.

*4.2.3.1. (2E)-1-(4-Chlorophenyl)-3-[3-methoxy-5-(prop-2-en-1-yl)-4-(prop-2-en-1-yloxy)phenyl]prop-2-en-1-one (**8**).* Yellow solid (Yield 74%); m.p. 69–71 °C; ^{1}H NMR ($CDCl_3$, 300 MHz): δ 8.02 (2H, d, J = 8.30 Hz), 7.71 (1H, s), 7.54–7.33 (3H, m), 7.15 (2H, d, J = 8.30 Hz), 6.11–5.99 (2H, m), 5.42–5.09 (4H, m), 4.59 (2H, d, J = 5.44 Hz), 3.93 (3H, s), 3.47 (2H, d, J = 6.50 Hz); ^{13}C NMR ($CDCl_3$, 75.4 MHz): δ 189.7, 153.4, 148.8, 145.8, 139.4, 137.1, 137.0, 135.0, 134.5, 130.8, 130.3, 129.3, 123.7, 121.0, 118.0, 116.8, 110.6, 74.3, 56.3 and 34.6. HRMS-ESI: m/z $[M + H]^+$ for $C_{22}H_{21}ClO_3$, calculated 369.6225; observed 369.6261.

*4.2.4. Procedure for the synthesis of chalcones **9**–**19** via **1b** (Table 2, Scheme 1)*

To a solution of **1b** (3 mmol) and appropriate acetophenone (3 mmol) in methanol (20 mL), 10% aqueous NaOH (4 mmol) was added. The remaining procedure for the synthesis of chalcones **9**–**19** was similar to that described above. The desired compounds obtained after recrystallization from MeOH and water was characterized by ^{1}H, ^{13}C NMR and HRMS data.

*4.2.4.1. (2E)-1-(4-Chlorophenyl)-3-[3-methoxy-4-(prop-2-en-1-yloxy)phenyl]prop-2-en-1-one (**9**).* Pale yellow solid (Yield 85%); m.p. 90–93 °C; FT-IR (KBr, cm^{-1}) 1657; ^{1}H NMR ($CDCl_3$, 300 MHz): δ 7.97 (2H, d, J = 8.45 Hz), 7.79 (1H, d, J = 15.56 Hz), 7.48 (2H, d, J = 8.45 Hz), 7.37 (1H, d, J = 15.56 Hz), 7.22–7.17 (2H, m), 6.92 (1H, d, J = 8.43 Hz), 6.15–6.03 (1H, m), 5.47 (2H, dd, J = 17.25, 10.45 Hz), 4.68(2H, d, J = 5.27 Hz), 3.95 (3H, s); ^{13}C NMR ($CDCl_3$, 75.4 MHz): δ 189.6, 151.1, 150.1, 145.9, 139.3, 137.2, 133.1, 130.2, 129.3, 128.3, 123.5, 119.9, 118.9, 113.4, 111.1, 70.2 and 56.5. HRMS-ESI: m/z $[M + H]^+$ for $C_{19}H_{17}ClO_3$, calculated 329.5913 observed 329.5932.

*4.2.4.2. (2E)-1-(3,4-Dichlorophenyl)-3-[3-methoxy-4-(prop-2-en-1-yloxy)phenyl]prop-2-en-1-one (**10**).* Light yellow solid (Yield 80%); m.p. 80–82 °C; ^{1}H NMR ($CDCl_3$, 300 MHz): δ 8.10 (1H, s), 7.86–7.77 (2H, m), 7.60 (1H, d, J = 8.00 Hz), 7.33–7.17 (3H, m), 6.93 (1H, d, J = 8.08 Hz), 6.15–6.04 (1H, m), 5.48 (2H, dd, J = 17.27, 10.46 Hz), 4.70 (2H, d, J = 4.17 Hz), 3.97 (3H, s); ^{13}C NMR ($CDCl_3$, 75.4 MHz): δ 188.4, 151.2, 150.0, 146.7, 138.5, 137.4, 133.6, 133.0, 131.1, 130.8, 128.0, 127.9, 123.8, 119.2, 118.9, 113.3, 110.9, 70.2 and 56.5. HRMS-ESI: m/z $[M + H]^+$ for $C_{19}H_{16}Cl_2O_3$, calculated 364.0362; observed 364.0328.

*4.2.4.3. (2E)-1-(4-Bromophenyl)-3-[3-methoxy-4-(prop-2-en-1-yloxy)phenyl]prop-2-en-1-one (**11**).* Yellow solid (Yield 80%); m.p. 100–103 °C; FT-IR (KBr, cm^{-1}) 1662; ^{1}H NMR ($CDCl_3$, 300 MHz): δ 7.90 (2H, d, J = 10.83 Hz), 7.79 (1H, d, J = 15.59 Hz), 7.66 (2H, d, J = 10.83 Hz), 7.36 (1H, d, J = 15.59 Hz), 7.23–7.16 (2H, m), 6.92 (1H, d, J = 8.30 Hz), 6.15–6.04 (1H, m), 5.47 (2H, dd, J = 17.26, 10.48 Hz), 4.69 (2H, d, J = 5.30 Hz), 3.96 (3H, s); ^{13}C NMR ($CDCl_3$, 75.4 MHz): δ 189.8, 151.0, 150.0, 145.9, 137.6, 133.0, 132.3, 130.4, 128.3, 128.0, 123.5, 119.8, 118.9, 113.3, 111.0, 70.2 and 56.5. HRMS-ESI: m/z $[M + H]^+$ for $C_{19}H_{17}O_3Br$, calculated 374.0426; observed 374.0453.

*4.2.4.4. (2E)-1-(4-Iodophenyl)-3-[3-methoxy-4-(prop-2-en-1-yloxy)phenyl]prop-2-en-1-one (**12**).* Pale orange solid (Yield 78%); m.p. 95–97 °C; ^{1}H NMR ($CDCl_3$, 300 MHz): δ 7.88–7.85 (2H, m), 7.79–7.70 (3H, m), 7.35 (1H, d, J = 15.59 Hz), 7.23–7.16 (2H, m), 6.92 (1H, d, J = 8.30 Hz), 6.17–6.04 (1H, m), 5.48 (2H, dd, J = 17.26, 10.47 Hz), 4.69 (2H, d, J = 5.31 Hz), δ 3.96 (3H, s); ^{13}C NMR ($CDCl_3$, 75.4 MHz): δ 190.1, 151.0, 150.0, 145.9, 138.3, 138.2, 133.1, 130.3, 128.3, 123.5, 119.9, 118.9, 113.3, 111.0, 100.7, 70.2 and 56.5. HRMS-ESI: m/z $[M + H]^+$ for $C_{19}H_{17}O_3I$, calculated 421.0431; observed 421.0418.

*4.2.4.5. (2E)-1-(4-Fluorophenyl)-3-[3-methoxy-4-(prop-2-en-1-yloxy)phenyl]prop-2-en-1-one (**13**).* Bright yellow solid (Yield 82%); m.p. 96–99 °C; ^{1}H NMR ($CDCl_3$, 300 MHz):δ 8.08 (2H, d, J = 8.40 Hz), 7.79 (1H, d, J = 15.56 Hz), 7.40 (1H, d, J = 15.56 Hz), 7.22–7.15 (4H, m), 6.92 (1H, d, J = 8.41 Hz), 6.15–6.04 (1H, m), 5.47 (2H, dd, J = 17.24, 10.49 Hz), 4.69 (2H, d, J = 5.28 Hz), 3.96 (3H, s); ^{13}C NMR ($CDCl_3$, 75.4 MHz): δ 189.3, 150.9, 150.0, 145.6, 135.2, 133.1, 131.3, 128.4, 123.4, 119.9, 118.8, 116.2, 115.9, 113.4, 111.0, 70.2 and 56.4. HRMS-ESI: m/z $[M + H]^+$ for $C_{19}H_{17}FO_3$, calculated 313.1370 observed 313.1343.

*4.2.4.6. (2E)-1-(3-Chlorophenyl)-3-[3-methoxy-4-(prop-2-en-1-yloxy)phenyl]prop-2-en-1-one (**14**).* Yellow solid (Yield 83%); m.p. 80–84 °C; ^{1}H NMR ($CDCl_3$, 300 MHz): δ 6.76 (1H, s), 6.66 (1H, d, J = 6.48 Hz), 6.58 (1H, dd, J = 5.44, 15.58 Hz), 6.31 (1H, d, J = 4.74 Hz), 6.23 (1H, d, J = 5.96 Hz), 6.13 (1H, dd, J = 5.44, 15.58 Hz), 6.00–5.93 (2H, m), 5.70(1H, t, J = 5.34 Hz), 4.92–4.79 (1H, m), 4.27–4.08 (2H, m), 3.45 (2H, s), 2.73 (3H, s); ^{13}C NMR ($CDCl_3$, 75.4 MHz): δ 188.3, 149.9, 148.8, 145.0, 139.3, 134.0, 131.8, 131.6, 129.1, 127.7, 126.9, 125.7, 122.4, 118.6, 117.7, 112.1, 109.7, 68.9 and 55.2. HRMS-ESI: m/z $[M + H]^+$ for $C_{19}H_{17}ClO_3$, calculated 329.5913; observed 329.5938.

*4.2.4.7. (2E)-1-(4-Methoxyphenyl)-3-[3-methoxy-4-(prop-2-en-1-yloxy)phenyl]prop-2-en-1-one (**15**).* Light orange solid (Yield 77%); m.p. 62–64 °C; ^{1}H NMR ($CDCl_3$, 300 MHz): δ 8.06 (2H, d, J = 8.68 Hz), 7.79 (1H, d, J = 15.55 Hz), 7.44 (1H, d, J = 15.55 Hz),

7.22–7.18 (2H, m), 7.00 (2H, d, $J = 8.68$ Hz), 6.89 (1H, d, $J = 4.93$ Hz), 6.16–6.03 (1H, m), 5.47 (2H, dd, $J = 17.26, 10.47$ Hz), 4.68 (2H, d, $J = 5.24$ Hz), 3.95 (3H, s), 3.89 (3H, s); ^{13}C NMR ($CDCl_3$, 75.4 MHz): δ 189.2, 163.7, 150.7, 149.9, 144.5, 133.2, 131.7, 131.1, 128.7, 123.1, 120.3, 118.8, 114.2, 113.4, 111.0, 70.1, 56.4 and 55.9. HRMS-ESI: m/z $[M + H]^+$ for $C_{20}H_{20}O_4$, calculated 325.1614; observed 325.1647.

*4.2.4.8. (2E)-1-(1,3-Benzodioxol-5-yl)-3-[3-methoxy-4-(prop-2-en-1-yloxy)phenyl]prop-2-en-1-one (**16**).* Creamish solid (Yield 79%); m.p. 86–89 °C; ^{1}H NMR ($CDCl_3$, 300 MHz): δ 7.76 (1H, d, $J = 15.52$ Hz), 7.66 (1H, d, $J = 8.26$ Hz), 7.52 (1H, s), 7.37 (1H, d, $J = 15.52$ Hz), 7.20–7.15 (2H, m), 6.90 (2H, d, $J = 8.26$ Hz), 6.13–6.02 (3H, m), 5.46 (2H, dd, $J = 15.20, 10.47$ Hz), 4.67–4.65 (2H, m), 3.94 (3H, s); ^{13}C NMR ($CDCl_3$, 75.4 MHz): δ 188.7, 151.9, 150.7, 149.9, 148.6, 144.8, 133.6, 133.2, 128.6, 124.9, 123.2, 120.1, 118.8, 113.3, 110.9, 108.8, 108.3, 102.2, 70.1 and 56.4. HRMS-ESI: m/z $[M + H]^+$ for $C_{20}H_{18}O_5$, calculated 339.1452; observed 339.1418.

*4.2.4.9. (2E)-3-[3-Methoxy-4-(prop-2-en-1-yloxy)phenyl]-1-(4-nitrophenyl)prop-2-en-1-one (**17**).* Orange solid (Yield 72%); m.p. 107–112 °C; ^{1}H NMR ($CDCl_3$, 3 00 MHz): δ 8.37 (2H, d, $J = 8.60$ Hz), 8.16 (2H, d, $J = 8.60$ Hz), 7.83 (1H, d, $J = 15.56$ Hz), 7.37 (1H, d, $J = 15.56$ Hz), 7.28–7.18 (2H, m), 6.94 (1H, d, $J = 8.29$ Hz), 6.15–6.04 (1H, m), 5.48 (2H, dd, $J = 17.24, 10.45$ Hz), 4.70 (2H, d, $J = 5.25$ Hz), 3.96 (3H, s); ^{13}C NMR ($CDCl_3$, 75.4 MHz): δ 189.4, 151.5, 150.3, 150.1, 147.4, 143.8, 132.9, 129.7, 127.9, 124.2, 123.9, 119.7, 118.9, 113.3, 111.1, 70.2 and 56.5. HRMS-ESI: m/z $[M + H]^+$ for $C_{19}H_{17}NO_5$, calculated 340.1405; observed 340.1451.

*4.2.4.10. (2E)-1-(4-Aminophenyl)-3-[3-methoxy-4-(prop-2-en-1-yloxy)phenyl]prop-2-en-1-one (**18**).* Bright yellow solid (Yield 70%); m.p. 103–107 °C; ^{1}H NMR ($CDCl_3$, 300 MHz): δ 8.38 (1H, d, $J = 8.25$ Hz), 8.11 (2H, d, $J = 8.25$ Hz), 7.82 (1H, d, $J = 15.20$ Hz), 7.62 (1H, s), 7.48 (1H, d, $J = 15.20$ Hz), 7.34–7.21 (3H, m), 6.98–6.72 (2H, m), 6.12–6.09 (1H, m), 5.48 (2H, dd, $J = 17.20, 10.25$ Hz), 4.70 (2H, d, $J = 5.30$ Hz), 3.96 (3H, s); ^{13}C NMR ($CDCl_3$, 75.4 MHz): δ 188.6, 151.7, 150.5, 149.9, 143.6, 133.2, 131.4, 128.9, 122.9, 120.5, 118.7, 114.3, 114.1, 113.5, 111.1, 70.2 and 56.4. HRMS-ESI: m/z $[M + H]^+$ for $C_{19}H_{19}NO_3$, calculated 310.1573; observed 310.1544.

*4.2.4.11. (2E)-3-[3-Methoxy-4-(prop-2-en-1-yloxy)phenyl]-1-phenylprop-2-en-1-one (**19**).* Yellow solid (Yield 88%); m.p. 78–81 °C; ^{1}H NMR ($CDCl_3$, 300 MHz): δ 8.04 (2H,d, $J = 8.15$ Hz), 7.80 (1H, d, $J = 15.63$ Hz), 7.59–7.49 (3H, m), 7.43 (1H, d, $J = 15.63$ Hz), 7.22–7.81 (2H, m), 6.93 (1H, d, $J = 8.15$ Hz), 6.15–6.04 (1H, m), 5.48 (2H, dd, $J = 17.26, 7.17$ Hz), 4.69–4.66 (2H, m), 3.96 (3H, s); ^{13}C NMR ($CDCl_3$, 75.4 MHz): δ 191.0, 150.9, 150.1, 145.4, 138.9, 133.2, 132.9, 128.9, 128.8, 128.5, 123.3, 120.6, 118.8, 113.4, 111.1, 70.2 and 56.5. HRMS-ESI: m/z $[M + H]^+$ for $C_{19}H_{18}O_3$, calculated 295.1464; observed 295.1438.

*4.2.5. Procedure for the synthesis of chalcone **20** via **5b** (Table 2, Scheme 2)*

To a 250-mL round bottom flask containing 4-hydroxyacetophenone (**2a**; 1.9 mmol) in dry acetone (20 mL), allyl bromide (2.0 mmol), and anhydrous K_2CO_3 (3.8 mmol) were added. The remaining procedure was similar to that described for **1b**. **5b** was obtained after column chromatography over silica gel. To a solution of **5b** (3 mmol), 10% aqueous NaOH (4 mmol) was added. Thereafter, **1b** (3 mmol) dissolved in 20 mL of methanol was added drop wise. The remaining procedure for the synthesis of chalcone **20** was similar to that described above.

*4.2.5.1. (2E)-3-[3-Methoxy-4-(prop-2-en-1-yloxy)phenyl]-1-[4-(prop-2-en-1-yloxy)phenyl] prop-2-en-1-one (**20**).* Light yellow solid (Yield 87%); m.p. 73–76 °C; ^{1}H NMR ($CDCl_3$, 300 MHz): δ 8.06 (2H, d, $J = 8.85$ Hz), 7.79 (1H, d, $J = 15.56$ Hz), 7.44 (1H, d, $J = 15.56$ Hz), 7.22–7.17 (2H, m), 7.02 (2H, d, $J = 8.85$ Hz), 6.92 (1H, d, $J = 8.22$ Hz), 6.15–6.04 (2H, m), 5.48 (4H, dd, $J = 16.20, 10.26$ Hz), 4.68 (4H, d, $J = 5.45$ Hz), 3.96 (3H, s); ^{13}C NMR ($CDCl_3$, 75.4 MHz): δ 189.1, 162.7, 150.7, 149.9, 144.5, 133.2, 132.9, 131.8, 131.1, 128.7, 123.1, 120.3, 118.8, 118.6, 114.9, 113.4, 110.9, 70.2, 69.3 and 56.4. HRMS-ESI: m/z $[M + H]^+$ for $C_{22}H_{22}O_4$, calculated 351.1770; observed 351.1739.

*4.2.6. Procedure for the synthesis of chalcones **21**, **22** via **6b**, **7b** (Table 3, Scheme 2)*

To a 250-mL round bottom flask containing substituted hydroxybenzaldehyde (**3a** or **4a**) (1.9 mmol) in dry acetone (20 mL), allyl bromide (2.0 mmol) and anhydrous K_2CO_3 (3.8 mmol) were added. The remaining procedure was similar to that described for **1b**. **6b** or **7b** (3 mmol) obtained after column chromatography over silica gel with hexane-ethyl acetate (9:1) was treated with 4-chloroacetophenone (3 mmol) and 10% aq. NaOH (4 mmol) in methanol (20 mL). The remaining procedure for chalcones **21** or **22** was similar to that described above and obtained compounds after recrystallization from MeOH and water were characterized by ^{1}H & ^{13}C NMR and HRMS data.

*4.2.6.1. (2E)-1-(4-Chlorophenyl)-3-[3-methoxy-2-(prop-2-en-1-yloxy)phenyl]prop-2-en-1-one (**21**).* Light yellow solid (Yield 77%); m.p. 70–75 °C; ^{1}H NMR ($CDCl_3$, 300 MHz): δ 8.14 (1H, d, $J = 15.89$ Hz), 7.98 (2H, d, $J = 8.54$ Hz), 7.60 (1H, d, $J = 15.89$ Hz), 7.50 (2H, d, $J = 6.70$ Hz), 7.29 (1H, d, $J = 7.80$ Hz), 7.14 (1H, t, $J = 8.03$ Hz), 7.01 (1H, d, $J = 8.10$ Hz), 6.16–6.05 (1H, m), 5.41 (2H, dd, $J = 17.15, 10.31$ Hz), 4.59 (2H, d, $J = 5.90$ Hz), 3.90 (3H, s); ^{13}C NMR ($CDCl_3$, 75.4 MHz): δ 190.1, 153.7, 148.1, 141.2, 139.4, 137.0, 134.2, 130.4, 129.6, 129.3, 124.6, 123.7, 120.4, 118.5, 114.8, 74.8 and 56.3. HRMS-ESI: m/z $[M + H]^+$ for $C_{19}H_{17}ClO_3$, calculated 329.5913; observed 329.5936.

*4.2.6.2. (2E)-1-(4-Chlorophenyl)-3-[4-methoxy-3-(prop-2-en-1-yloxy)phenyl]prop-2-en-1-one (**22**).* Light yellow solid (Yield 84%); m.p. 80–83 °C; ^{1}H NMR ($CDCl_3$, 300 MHz): δ 7.99 (2H, d, $J = 8.31$ Hz), 7.73 (1H, d, $J = 15.31$ Hz), 7.51 (2H, d, $J = 8.31$ Hz), 7.35–7.19 (3H, m), 6.94 (1H, d, $J = 15.31$ Hz), 6.13–6.04 (1H, m), 5.48–5.29 (2H, m), 4.72 (2H, d, $J = 10.29$ Hz), 3.94 (3H, s); ^{13}C NMR ($CDCl_3$, 75.4 MHz): δ 189.6, 152.5, 148.7, 145.4, 139.4, 137.2, 133.4, 130.2, 129.3, 128.0, 123.9, 119.8, 118.8, 113.0, 112.0, 70.4 and 56.4. HRMS-ESI: m/z $[M + H]^+$ for $C_{19}H_{17}ClO_3$, calculated 329.5913; observed 329.5941.

*4.2.7. Procedure for the synthesis of chalcone **23** (Table 3, Scheme 3)*

To the solution of vanillin (3 mmol) and chloroacetophenone (3 mmol) in ethanol (20 mL), KOH (4 mmol) was added. The remaining procedure was similar to that described for other chalcones. Compound **23** obtained after recrystallization was characterized by NMR and HRMS data.

*4.2.7.1. (2E)-1-(4-Chlorophenyl)-3-(4-hydroxy-3-methoxyphenyl) prop-2-en-1-one (**23**).* Bright yellow solid (Yield 60%); m.p. 110–115 °C; ^{1}H NMR ($CDCl_3$, 300 MHz): δ 7.98 (2H, d, $J = 8.50$ Hz), 7.79 (1H, d, $J = 15.57$ Hz), 7.49 (2H, d, $J = 8.50$ Hz), 7.36 (1H, d, $J = 15.57$ Hz), 7.24 (1H, dd, $J = 1.30, 1.27$ Hz), 7.13 (1H, s), 6.99 (1H, d, $J = 8.20$ Hz), 6.11 (1H, s), 3.97 (3H, s); ^{13}C NMR ($CDCl_3$, 75.4 MHz): δ 189.7, 148.9, 147.3, 146.2, 139.4, 137.2, 130.2, 129.3, 127.7, 123.9, 119.6, 115.4, 110.5 and 56.4. HRMS-ESI: m/z $[M + H]^+$ for $C_{16}H_{13}ClO_3$, calculated 289.5601; observed 289.5627.

*4.2.8. Procedure for the synthesis of chalcones **24**–**26** (Table 3, Scheme 3)*

To a 250 mL round bottom flask containing 1-(4-chlorophenyl)-3-(4-hydroxy-3-methoxyphenyl)prop-2-en-1-one (**23**) (1.9 mmol) in dry acetone (20 mL), prenyl bromide (for **24**) or 1-bromobutane (for **25**) or 4-bromobenzyl bromide (for **26**) (2.0 mmol each) and anhydrous K_2CO_3 (3.8 mmol) were added. The remaining procedure was similar to as described above. The desired compounds **24**–**26** obtained after column chromatography over silica gel with hexane-ethyl acetate (9:1) was characterized by ^1H & ^{13}C NMR and HRMS data.

*4.2.8.1. (2E)-1-(4-Chlorophenyl)-3-{3-methoxy-4-[(3-methylbut-2-en-1-yl)oxy]phenyl}prop-2-en-1-one (**24**).* Yellow solid (Yield 62%); m.p. 71–74 °C; ^1H NMR ($CDCl_3$, 300 MHz): δ 7.79–7.95 (2H, m), 7.82 (1H, dd, *J* = 7.79, 15.52 Hz), 7.50–7.46 (2H, m), 7.39 (1H, dd, *J* = 7.80, 15.55 Hz), 7.29–7.16 (2H, m), 6.93 (1H, s), 5.52 (1H, s), 4.66 (2H, s), 3.96 (3H, d, *J* = 4.85 Hz), 1.78 (6H, s); ^{13}C NMR ($CDCl_3$, 75.4 MHz): δ 189.7, 151.4, 150.0, 146.1, 139.3, 137.2, 130.7, 130.3, 129.3, 127.9, 123.6, 119.7, 113.0, 112.0, 110.7, 66.2, 56.4, 26.3 and 18.7. HRMS-ESI: *m*/*z* [M + H]$^+$ for $C_{21}H_{21}ClO_3$, calculated 357.6225; observed 357.5643.

*4.2.8.2. (2E)-3-(4-Butoxy-3-methoxyphenyl)-1-(4-chlorophenyl) prop-2-en-1-one (**25**).* Yellow solid (Yield 81%); m.p. 47–50 °C; ^1H NMR ($CDCl_3$, 300 MHz): δ 7.99 (2H, d, *J* = 8.44 Hz), 7.81 (1H, d, *J* = 15.60 Hz), 7.50 (2H, d, *J* = 8.43 Hz), 7.37 (1H, d, *J* = 15.55 Hz), 7.26–7.18 (2H, m), 6.93 (1H, d, *J* = 8.30 Hz), 4.11 (2H, t), 3.95 (3H, s), 1.89–1.83 (2H, m), 1.57–1.49 (2H, m), 1.01 (3H, t); ^{13}C NMR ($CDCl_3$, 75.4 MHz): δ 189.7, 151.8, 149.9, 146.1, 139.3, 137.2, 130.2, 129.3, 127.9, 123.8, 119.7, 112.8, 111.1, 69.1, 56.5, 31.5, 19.6 and 14.2. HRMS-ESI: *m*/*z* [M + H]$^+$ for $C_{20}H_{21}ClO_3$, calculated 345.6225; observed 345.6203.

*4.2.8.3. (2E)-3-{4-[(4-Bromobenzyl)oxy]-3-methoxyphenyl}-1-(4-chlorophenyl)prop-2-en-1-one (**26**).* Creamish solid (Yield 75%); m.p. 115–120 °C; ^1H NMR ($CDCl_3$, 300 MHz): δ 7.98 (2H, d, *J* = 8.47 Hz), 7.78 (1H, d, *J* = 15.57 Hz), 7.53–7.46 (4H, m), 7.37–7.28 (3H, m), 7.18 (2H, d, *J* = 5.46 Hz), 6.89 (1H, *d*, *J* = 8.77 Hz), 5.15 (2H, s), 3.96 (3H, s); ^{13}C NMR ($CDCl_3$, 75.4 MHz): δ 189.6, 150.8, 150.2, 145.7, 139.4, 137.1, 135.9, 132.2, 130.3, 129.3, 128.7, 123.3, 122.4, 120.1, 113.9, 111.3, 70.6 and 56.4. HRMS-ESI: *m*/*z* [M + H]$^+$ for $C_{23}H_{18}ClBrO_3$, calculated 458.5031; observed 458.5054.

*4.2.9. Procedure for the synthesis of chalcones **27**–**32** via **8b**–**13b** (Table 3, Scheme 4)*

To a 250 mL round bottom flask containing substituted hydroxybenzaldehyde (**5a** or **6a** or **7a** or **8a** or **9a** or **10a**) (1.9 mmol) in dry acetone (20 mL), allyl bromide (2.0 mmol) and anhydrous K_2CO_3 (3.8 mmol) were added. The remaining procedure was similar to that described for **1b**. Compound **8b**–**13b** obtained, respectively after column chromatography over silica gel with hexane-ethyl acetate (9:1) was treated with 4-chloroacetophenone (3 mmol) in methanol (20 mL) and 10% aqueous NaOH (4 mmol). The remaining procedure was similar to as described above. The desired compound **27**–**32** obtained after recrystallization from MeOH and water was characterized by ^1H & ^{13}C NMR and HRMS data.

*4.2.9.1. (2E)-1-(4-Chlorophenyl)-3-[3,5-dimethoxy-4-(prop-2-en-1-yloxy)phenyl]prop-2-en-1-one (**27**).* Yellow solid (Yield 76%); m.p. 120–123 °C; ^1H NMR ($CDCl_3$, 300 MHz): δ 7.99 (2H,d, *J* = 8.53 Hz), 7.52 (1H, d, *J* = 15.60 Hz), 7.50 (2H, d, *J* = 8.53 Hz), 7.38 (1H, d, *J* = 15.60 Hz), 6.86 (2H, s), 6.16–6.06 (1H, m), 5.37–5.20 (2H, m), 4.61 (2H, d, *J* = 5.20 Hz), 3.91 (6H, s); ^{13}C NMR ($CDCl_3$, 75.4 MHz): δ 189.6, 154.1, 145.9, 139.7, 139.5, 136.9, 134.5, 130.6, 130.3, 129.3, 121.2, 118.5, 106.2, 74.7 and 56.6. HRMS-ESI: *m*/*z* [M + H]$^+$ for $C_{20}H_{19}ClO_4$, calculated 359.6063; observed 359.6042.

*4.2.9.2. (2E)-1-(4-Chlorophenyl)-3-[4-(prop-2-en-1-yloxy)phenyl] prop-2-en-1-one (**28**).* Light yellow solid (Yield 90%); m.p. 101–104 °C; ^1H NMR ($CDCl_3$, 300 MHz): δ 7.99 (2H,d, *J* = 8.73 Hz), 7.82 (1H, d, *J* = 15.60 Hz), 7.62 (2H, d, *J* = 8.73 Hz), 7.50 (2H, d, *J* = 8.73 Hz), 7.40 (1H, d, *J* = 15.60 Hz), 6.99 (2H, d, *J* = 8.73 Hz), 6.14–6.01 (1H, m), 5.47(2H, dd, *J* = 18.78, 10.5 Hz), 4.61–4.59 (2H, m); ^{13}C NMR ($CDCl_3$, 75.4 MHz): δ 189.6, 161.3, 145.6, 139.3, 137.2, 133.1, 130.7, 130.2, 129.3, 127.9, 119.7, 118.5, 115.6 and 51.2. HRMS-ESI: *m*/*z* [M + H]$^+$ for $C_{18}H_{15}ClO_2$, calculated 299.5763; observed 299.5738.

*4.2.9.3. (2E)-1-(4-Chlorophenyl)-3-[2-(prop-2-en-1-yloxy)phenyl] prop-2-en-1-one (**29**).* Creamish solid (Yield 78%); m.p. 91–93 °C; ^1H NMR ($CDCl_3$, 300 MHz): δ 8.19 (1H, d, *J* = 15.39 Hz), 7.99 (2H, d, *J* = 6.80 Hz), 7.68 (2H, d, *J* = 6.87 Hz), 7.50 (2H, d, *J* = 6.87 Hz), 7.41 (1H, d, *J* = 15.39 Hz), 7.05–6.95 (2H, m), 6.18–6.08 (1H, m), 5.51 (2H, dd, *J* = 17.23, 10.45 Hz), 4.66 (2H, s); ^{13}C NMR ($CDCl_3$, 75.4 MHz): δ 190.5, 158.6, 141.7, 139.7, 137.6, 133.5, 132.6, 130.7, 130.4, 129.6, 124.7, 123.2, 121.7, 118.8, 113.3 and 69.9. HRMS-ESI: *m*/*z* [M + H]$^+$ for $C_{18}H_{15}ClO_2$, calculated 299.5763; observed 299.5746.

*4.2.9.4. (2E)-1-(4-Chlorophenyl)-3-[3-ethoxy-4-(prop-2-en-1-yloxy) phenyl]prop-2-en-1-one (**30**).* Light yellow solid (Yield 88%); m.p. 85–89 °C; ^1H NMR ($CDCl_3$, 300 MHz): δ 7.89 (2H, d, *J* = 8.23 Hz), 7.78 (1H, d, *J* = 15.52 Hz), 7.36 (2H, d, *J* = 8.23 Hz), 7.31 (1H, d, *J* = 15.52 Hz), 7.21 (2H, d, *J* = 7.67 Hz), 6.92 (1H, s), 6.11–6.05 (1H, m), 5.47–5.31 (2H, m), 5.31 (2H, s), 4.18 (2H, d, *J* = 6.82 Hz), 1.53 (3H, t); ^{13}C NMR ($CDCl_3$, 75.4 MHz): δ 189.6, 151.5, 149.4, 145.9, 139.3, 137.2, 133.3, 130.2, 129.3, 128.3, 123.5, 119.8, 118.4, 113.9, 113.0 70.2, 65.2 and 15.2. HRMS-ESI: *m*/*z* [M + H]$^+$ for $C_{20}H_{19}ClO_3$, calculated 343.6069; observed 343.6034.

*4.2.9.5. (2E)-3-[3,4-Bis(prop-2-en-1-yloxy)phenyl]-1-(4-chlorophenyl)prop-2-en-1-one (**31**).* Light yellow solid (Yield 90%); m.p. 72–75 °C; FT-IR (KBr, cm^{-1}) 1658; ^1H NMR ($CDCl_3$, 300 MHz): δ 7.99 (2H, d, *J* = 7.83 Hz), 7.79 (1H, d, *J* = 15.54 Hz), 7.51 (2H, d, *J* = 6.16 Hz), 7.37 (1H, d, *J* = 15.54 Hz), 7.20 (2H, d, *J* = 7.83 Hz), 6.94 (1H, s), 6.13–6.09 (2H, m), 5.50–5.33 (4H, m), 4.69 (4H, s); ^{13}C NMR ($CDCl_3$, 75.4 MHz): δ 189.6, 151.6, 149.0, 145.8, 139.6, 137.2, 133.5, 133.2, 130.2, 129.3, 128.3, 123.8, 119.9, 118.5, 118.4, 113.9, 113.7, 70.5 and 70.1. HRMS-ESI: *m*/*z* [M + H]$^+$ for $C_{21}H_{19}ClO_3$, calculated 355.6069; observed 355.6069.

*4.2.9.6. (2E)-3-(4-Chlorophenyl)-1-[3-methoxy-4-(prop-2-en-1-yloxy)phenyl]prop-2-en-1-one (**32**).* Light yellow solid (Yield 80%); m.p. 120–123 °C; ^1H NMR ($CDCl_3$, 300 MHz): δ 7.79 (1H,d, *J* = 15.63 Hz), 7.67–7.64 (2H, m), 7.59–7.55 (3H, m), 7.40 (2H, d, *J* = 8.18 Hz), 6.95 (1H, d, *J* = 8.18 Hz), 5.49–5.18 (1H, m), 5.49 (2H, dd, *J* = 17.25, 10.47 Hz), 4.73–4.70 (2H, m), 3.98 (3H, s); ^{13}C NMR ($CDCl_3$, 75.4 MHz): δ 188.6, 152.8, 150.0, 142.8, 136.6, 133.9, 132.9, 131.7, 129.9, 129.6, 123.3, 122.5, 119.0, 112.0, 111.5, 70.2 and 56.5. HRMS-ESI: *m*/*z* [M + H]$^+$ for $C_{19}H_{17}ClO_3$, calculated 329.5913; observed 329.5929.

*4.2.10. General procedure for the synthesis of heterocyclic chalcone derivatives **33**–**38** (Table 4, Scheme 5)*

To a solution of **1b** (3 mmol) and appropriate aceto derivative (3 mmol) in methanol (20 mL), 10% aq. NaOH (4 mmol) was added. The remaining procedure was similar to that described for the synthesis of chalcones. Compounds **33**–**38** obtained after

recrystallization from MeOH and water were characterized by ^{1}H &^{13}C NMR and HRMS data.

*4.2.10.1. (2E)-1-(Furan-2-yl)-3-[3-methoxy-4-(prop-2-en-1-yloxy) phenyl]prop-2-en-1-one (**33**).* Light yellow solid (Yield 70%); m.p. 132–135 °C; ^{1}H NMR ($CDCl_3$, 300 MHz): δ 7.82 (1H, d, J = 15.81 Hz), 7.29–7.11 (5H, m), 6.91 (1H, d, J = 8.36 Hz), 6.38 (1H, d, J = 5.80 Hz), 6.13–6.02 (1H, m), 5.46 (2H, dd, J = 17.26, 10.47 Hz), 4.67 (2H, d, J = 5.20 Hz), 3.95 (3H, s); ^{13}C NMR ($CDCl_3$, 75.4 MHz): δ 179.5, 150.6, 150.0, 142.7, 133.7, 133.3, 128.7, 126.0, 122.9, 120.6, 118.7, 116.7, 113.5, 111.3, 111.2, 70.2 and 56.5. HRMS-ESI: m/z $[M + H]^+$ for $C_{17}H_{16}O_4$, calculated 285.1302; observed 285.1345.

*4.2.10.2. 3-{(2E)-3-[3-Methoxy-4-(prop-2-en-1-yloxy)phenyl]prop-2-enoyl}-2H-chromen-2-one (**34**).* Yellow solid (Yield 70%); m.p. 148–151 °C; ^{1}H NMR ($CDCl_3$, 300 MHz): δ 8.58 (1H, s), 7.82 (2H, s), 7.69 (2H, d, J = 7.44 Hz), 7.41–7.33 (2H, m), 7.27 (2H, d, J = 8.58 Hz), 6.91(1H, d, J = 7.44 Hz), 6.14–6.07 (1H, m), 5.47 (2H, dd, J = 17.22, 10.26 Hz), 4.68 (2H, s), 3.95 (3H, s); ^{13}C NMR ($CDCl_3$, 75.4 MHz): δ 186.6, 159.8, 155.6, 151.2, 149.9, 148.2, 145.7, 134.5, 133.1, 130.2, 128.5, 126.0, 125.3, 124.1, 122.3, 119.0, 118.9, 117.0, 113.2, 111.1, 70.1 and 56.4. HRMS-ESI: m/z $[M + H]^+$ for $C_{22}H_{18}O_5$, calculated 363.1452; observed 363.1433.

*4.2.10.3. 4-Hydroxy-3-{(2E)-3-[3-methoxy-4-(prop-2-en-1-yloxy) phenyl]prop-2-enoyl}-2H-chromen-2-one (**35**).* Orange solid (Yield 68%); m.p. 150–153 °C; ^{1}H NMR ($CDCl_3$, 300 MHz): δ 8.30 (1H, d, J = 15.34 Hz), 8.10 (1H, d, J = 7.62 Hz), 8.00 (1H, d, J = 15.34 Hz), 7.68–7.63 (1H, m), 7.42–7.23 (4H, m), 6.91 (1H, d, J = 8.15 Hz), 6.14–6.07 (1H, m), 5.47 (2H, dd, J = 17.20, 10.25 Hz), 4.72 (2H, d, J = 5.20 Hz), 3.96 (3H, s), 3.09 (1H, s); ^{13}C NMR ($CDCl_3$, 75.4 MHz): δ 181.7, 161.6, 154.9, 151.6, 150.1, 147.2, 145.5, 135.8, 133.0, 128.5, 126.2, 124.7, 124.6, 121.5, 118.9, 117.8, 117.3, 113.2, 111.4, 101.3, 70.2 and 56.4. HRMS-ESI: m/z $[M + H]^+$ for $C_{22}H_{18}O_6$, calculated 379.1446; observed 379.1426.

*4.2.10.4. (2E)-3-[3-Methoxy-4-(prop-2-en-1-yloxy)phenyl]-1-(1H-pyrrol-2-yl)prop-2-en-1-one (**36**).* Light yellow solid (Yield 63%); m.p. 132–135 °C; ^{1}H NMR ($CDCl_3$, 300 MHz): δ 9.81 (1H, s), 7.84 (1H, d, J = 15.85 Hz), 7.29–7.12 (5H, m), 6.91 (1H, d, J = 8.40 Hz), 6.36–6.33 (1H, m), 6.15–6.03 (1H, m), 5.46 (2H, dd, J = 17.26, 10.47 Hz), 4.67 (2H, d, J = 5.31 Hz), 3.95 (3H, s); ^{13}C NMR ($CDCl_3$, 75.4 MHz): δ 179.5, 150.6, 150.0, 142.7, 133.7, 133.2, 128.7, 125.9, 125.9, 120.5, 118.7, 116.7, 113.5, 111.2, 70.2 and 56.5. HRMS-ESI: m/z $[M + H]^+$ for$C_{17}H_{17}NO_3$, calculated 284.1417; observed 284.1442.

*4.2.10.5. 5-[3-Methoxy-4-(prop-2-en-1-yloxy)benzylidene]-2,2-dimethyl-1,3-dioxane-4,6-dione (**37**).* Fluorescent yellow solid (Yield 91%); m.p. 128–133 °C; ^{1}H NMR ($CDCl_3$, 300 MHz): δ 8.34 (1H, s), 8.29 (1H, s), 7.63 (1H, d, J = 8.52 Hz), 6.95 (1H, d, J = 8.52 Hz), 6.08–6.03 (1H, m), 5.46–5.33 (2H, m), 4.74 (2H, d, J = 5.37 Hz), 3.95 (3H, s), 1.79 (6H, s); ^{13}C NMR ($CDCl_3$, 75.4 MHz): δ 164.6, 161.0, 158.6, 154.2, 149.4, 132.7, 132.4, 125.5, 119.4, 116.5, 112.4, 111.0, 104.6, 70.2, 56.4 and 27.8. HRMS-ESI: m/z $[M + H]^+$ for $C_{17}H_{18}O_6$, calculated 319.1446; observed 319.1479.

*4.2.10.6. 5-[3-Methoxy-4-(prop-2-en-1-yloxy)benzylidene]pyrimidine-2,4,6(1H,3H,5H)-trione (**38**).* Bright yellow solid (Yield 90%); m.p. 250–256 °C; ^{1}H NMR (DMSO-d_6, 300 MHz): δ 9.99 (1H, s), 9.87 (1H, s), 7.06 (1H, s), 6.91 (1H, s), 6.49 (1H, d, J = 8.32 Hz), 5.78 (1H, d, J = 8.36 Hz), 4.12–3.97 (1H, m), 4.12–3.97 (2H, m), 3.37 (2H, d, J = 3.39 Hz), 2.31 (3H, s); ^{13}C NMR (DMSO-d_6, 75.4 MHz): δ 164.2, 162.4, 155.9, 152.7, 150.4, 148.0, 132.9, 131.7, 125.4, 118.6, 116.9, 115.2, 112.3, 69.1 and 55.6.HRMS-ESI: m/z $[M + H]^+$ for $C_{15}H_{14}N_2O_5$, calculated 303.1202; observed 303.1149.

*4.2.11. Procedure for the synthesis of heterocyclic chalcone derivative **39** (Table 4, Scheme 5)*

To a solution of 4,7-dichloroquinoline (2.5 mmol) in tetrahydrofuran (20 mL), compound **18** (2.75 mmol) was added and the mixture was refluxed for 8 h. Thereafter the reaction mixture was cooled and thus formed precipitates were filtered, washed with water, diethyl ether and recrystallized from alcohol. The desired compound obtained after recrystallization from MeOH and water was characterized by ^{1}H & ^{13}C NMR and HRMS data.

*4.2.11.1. (E)-3-(4-(Allyloxy)-3-methoxyphenyl)-1-(4-((7-chloroquinolin-4-yl)amino)phenyl)prop-2-en-1-one (**39**).* Yellow solid (Yield 76%); m.p. 168–171 °C; ^{1}H NMR ($CDCl_3$ + DMSO-d_6, 300 MHz): δ 7.35 (2H, d, J = 8.41 Hz), 6.93 (2H, d, J = 7.83 Hz), 6.78 (1H, s), 6.60 (1H, s), 6.50–6.29 (4H, m), 6.08 (1H, s), 6.02 (1H, d, J = 7.8 Hz), 5.92 (1H, d, J = 4.82 Hz), 5.71 (1H, d, J = 8.42 Hz), 4.84–4.76 (1H, m), 4.20 (2H, dd, J = 15.34, 10.52 Hz), 3.39 (2H, d, J = 5.10 Hz), 2.68 (3H, s); ^{13}C NMR ($CDCl_3$ + DMSO-d_6, 75.4 MHz): δ 188.8, 151.5, 150.9, 150.1, 149.6, 147.9, 145.1, 144.9, 143.9, 137.9, 135.1, 133.4, 130.8, 128.5, 127.5, 125.7, 124.1, 123.9, 122.7, 120.2, 118.6, 113.7, 111.5, 103.4, 69.9 and 56.6. HRMS-ESI: m/z $[M + H]^+$ for $C_{28}H_{23}ClN_2O_3$, calculated 471.6443; observed 471.6421.

*4.2.12. Procedure for the synthesis of heterocyclic chalcone derivative **40** (Table 4, Scheme 5)*

To the solution of compound **39** (2.7 mmol) in dry tetrahydrofuran (15 mL), KOH (13.5 mmol), allyl bromide (5.5 mmol) and cetyltrimethylammonium bromide (CTAB) (0.7 mmol) was added. The contents were stirred at rt for 12–14 h till the starting disappeared (monitored by TLC). After the completion of reaction, the reaction mixture was partitioned between ethyl acetate (70 mL) and water (15 mL). The ethyl acetate layer was washed with water till neutral, dried over sodium sulfate and evaporated. The obtained residue was purified by column chromatography (silica gel, hexane: ethyl acetate (7:3 v/v)) to afford **40** whose structure was confirmed through NMR and mass spectrometry.

*4.2.12.1. (E)-1-(4-(Allyl(7-chloroquinolin-4-yl)amino)phenyl)-3-(4-(allyloxy)-3-methoxyphenyl)prop-2-en-1-one (**40**).*
Orange-yellow viscous liquid (Yield 61%); ^{1}H NMR ($CDCl_3$, 300 MHz): δ 7.40 (2H, d, J = 8.30 Hz), 6.92 (2H, d, J = 7.80 Hz), 6.73 (1H, s), 6.56 (1H, s), 6.49–6.30 (4H, m), 6.06 (1H, s), 6.05 (1H, d, J = 7.80 Hz), 5.90 (1H, d, J = 4.85 Hz), 5.70 (1H, d, J = 8.40 Hz), 4.80–4.75 (2H, m), 4.19–4.02 (4H, m), 3.40 (2H, d, J = 5.10 Hz), 3.30 (2H, d, J = 5.11 Hz), 2.60 (3H, s); ^{13}C NMR ($CDCl_3$, 75.4 MHz): δ 188.9, 151.4, 151.0, 150.0, 149.5, 147.7, 145.0, 144.7, 143.7, 137.6, 136.0, 135.0, 133.6, 130.7, 128.6, 127.7, 125.1, 124.0, 123.7, 122.7, 120.2, 118.4, 116.2, 113.7, 111.5, 103.4, 70.0, 56.3 and 44.5. HRMS-ESI: m/z $[M + H]^+$ for $C_{31}H_{27}ClN_2O_3$, calculated 511.6755; observed 511.6736.

*4.2.13. Procedure for the synthesis of heterocyclic chalcone derivative **41** (Table 4, Scheme 5)*

In a 100 mL round bottom flask, mixture of **9** (1.5 mmol), phenylhydrazine hydrochloride (4.5 mmol) and sodium acetate (0.25 mmol) was taken. To this mixture, added 15 mL of aq. acetic acid (HAc/H_2O; 2:1) and refluxed the contents for 8–10 h till the starting was consumed (monitored by TLC). Thereafter the reaction mixture was cooled and poured in ice cold water. The obtained precipitates were filtered, washed with water till neutral pH and recrystallized from alcohol to afford **41**.

*4.2.13.1. 5-(4-(Allyloxy)-3-methoxyphenyl)-3-(4-chlorophenyl)-1-phenyl-4,5-dihydro-1H-pyrazole (**41**).* Creamish solid (Yield 60%); m.p. 116–121 °C; FT-IR (KBr, cm^{-1}) 1668; ^{1}H NMR ($CDCl_3$, 300 MHz): δ 7.68 (2H, dd, J = 1.69, 1.70 Hz), 7.38 (2H, dd, J = 1.71,

1.67 Hz), 7.24–7.18 (2H, m), 7.11 (2H, d, J = 8.22 Hz), 6.86 (4H, d, J = 6.03 Hz), 6.17–6.06 (1H,m), 5.44–5.28 (2H, m), 4.62 (2H, d, J = 4.46), 3.83 (3H, s), 3.17 (1H, t, J = 1.50 Hz), 1.60 (2H, s); ^{13}C NMR ($CDCl_3$, 75.4 MHz): δ 150.5, 147.9, 146.1, 145.3, 135.7, 134.7, 133.7, 131.7, 129.3, 129.2, 127.3, 119.9, 118.4, 114.0, 109.5, 70.3, 65.2, 56.4 and 43.9. HRMS-ESI: m/z $[M + H]^+$ for $C_{25}H_{23}ClN_2O_2$, calculated 419.1759; observed 419.1722.

4.2.14. Procedure for the synthesis of heterocyclic chalcone derivative **42** (Table 4, Scheme 5)

In a 100 mL round bottom flask, mixture of **9** (1.5 mmol), guanidine hydrochloride (1.5 mmol) and KOH (5 mmol) was taken in ethanol (25 mL). The contents were refluxed for 6 h till the starting was consumed (monitored by TLC). Thereafter, the organic layer was evaporated *in vacuo* and the product was recrystallized from hexane-alcohol system whose structure was confirmed through NMR and mass spectrometry.

4.2.14.1. 4-(4-(Allyloxy)-3-methoxyphenyl)-6-(4-chlorophenyl)pyrimidin-2-amine (**42**).

Creamish solid (Yield 82%); m.p. 184–186 °C; ^{1}H NMR ($CDCl_3$, 300 MHz): δ 8.02 (2H, d, J = 7.73 Hz), 7.72 (1H, s), 7.61 (1H, d, J = 8.43), 7.49(2H, d, J = 7.73 Hz), 7.38 (1H, s), 6.99 (1H, d, J = 8.31 Hz), 6.17–6.06 (1H, m), 5.48–5.29 (4H, m), 4.71 (2H, d, J = 4.46 Hz), 4.01 (3H, s); ^{13}C NMR ($CDCl_3$, 75.4 MHz): δ 166.3, 165.1, 163.9, 150.7, 150.0, 136.9, 136.7, 133.3, 130.9, 129.4, 128.8, 120.4, 118.8, 113.2, 110.7, 103.7, 70.2 and 56.5. HRMS-ESI: m/z $[M + H]^+$ for $C_{20}H_{18}ClN_3O_2$, calculated 368.6090; observed 368.6063.

4.3. Measurement of inhibition of P. falciparum growth in culture

CQ sensitive *Pf*3D7 and chloroquine resistant *Pf*Dd2 and *Pf*INDO strains were cultivated *in vitro* by the method of Trager and Jensen [80] with minor modifications. Cultures were maintained in fresh O^+ human erythrocytes at 4% hematocrit in complete medium (RPMI 1640 with 0.2% sodium bicarbonate, 0.5% Albumax, 45 mg L^{-1} hypoxanthine and 50 mg L^{-1} gentamicin) at 37 °C under reduced O_2 (gas mixture 5% O_2, 5% CO_2, and 90% N_2). Stock solutions of **CQ** were prepared in water (milliQ grade). ART and test compounds were dissolved in DMSO. All stocks were then diluted with culture medium to achieve the required concentrations (in all cases the final concentration contained 0.4% DMSO, which was found to be non-toxic to the parasite). Antimalarial drugs and test compounds were then placed in 96-well flat-bottom tissue culture grade plates to yield triplicate wells with drug concentrations ranging from 0 to 100 μM in a final well volume of 100 μL for primary screening. Chloroquine 100 nM and 1000 nM were used as positive controls for *Pf*3D7 and *Pf*INDO strains respectively. The antiplasmodial activities of allylated chalcones were measured by fluorescence based SYBR Green I assay [47]. Parasite culture was synchronized at ring stage with 5% sorbitol [81]. Synchronized culture was aliquoted to a drug containing 96-well plates at 2% hematocrit and 1% parasitemia. After 48 h of incubation under standard culture conditions, plates were harvested and read by the SYBR Green I fluorescence-based method using a 96-well fluorescence plate reader (Victor, Perkin Elmer), with excitation and emission wavelengths at 485 and 530 nm, respectively. The fluorescence readings were plotted against drug concentration, and IC_{50} values obtained by visual matching of the drug concentration giving 50% inhibition of growth.

4.4. Measurement of cytotoxic activity against mammalian cell lines in culture

MTT assay for mammalian cell viability assay as described by Mosmann [82] was used to determine drug induced cytotoxicity against HeLa and fibroblast L929 cells cultured in complete RPMI containing 10% fetal bovine serum, 0.2% sodium bicarbonate and 50 μg mL^{-1} gentamicin. Briefly, cells (10^4 cells/200 μL/well) were seeded into 96-well flat-bottom tissue-culture plates in complete culture medium. Chalcone stock solutions were made in DMSO and diluted to the desired concentrations in cRPMI. The final concentration of DMSO during incubation with mammalian cells was 0.4% which was found to be non toxic to the cells. Drugs were added after overnight seeding and incubated for 24 h in a humidified atmosphere at 37 °C and 5% CO_2. DMSO (final concentration 10%) was added as +ve control. An aliquot of a stock solution of 3-(4,5-dimethylthiazol-2-yl)-2,5-diphenyltetrazolium bromide (MTT) (5 mg mL^{-1} in 1X phosphate buffered saline) was added at 20 μL per well, and incubated for another 3 h. After spinning the plate (1500 RPM for 5 min), supernatant was removed and 100 μL of the stop agent DMSO was added to each well. Formation of formazon, an index of growth, was read at 570 nm by 96-well plate reader (Versa Max), and IC_{50} values were determined by analysis of dose–response curves. Selectivity index was calculated as IC_{50} mammalian cell/IC_{50} P*f*3D7.

4.5. Preparation of drug combinations

For the combination studies, the 8X IC_{50} stock solutions and dilutions of individual compounds (**CQ**: 320 nM, **ART**: 120 nM, **9**: 20 μM (for P*f*3D7); **CQ**: 3500 nM, **ART**: 120 nM, **9**: 130 μM (for P*f*INDO)) were prepared in complete RPMI. Stock solutions of **CQ**/**ART** were then combined with stock solutions of **9** in the volumetric ratios of 1:0, 1:1, 1:2, 2:1, 1:3, 3:1, 1:5 and 0:1 (Table S7, see SI). The stock mixtures of each of the two drugs (32 in all) were placed into the wells of sterile 96 wells plate and serially two fold diluted. Finally the above mentioned stocks and their respective dilutions were transferred into 96 well flat-bottomed cell culture plates to give triplicates of each combination dose.

4.6. Data analysis

To study the effect of each combination, IC_{50} values were determined for individual drugs (**ART**, **CQ**, **9**) and for a series of drug combinations (**ART** + **9**, **CQ** + **9**). The IC_{50}s obtained were used to derive 50% Fractional inhibitory concentration (FIC_{50}) values of each drug by using following equation.

$$\mathbf{FIC_{50} = IC_{50}\ for\ drug\ in\ combination / IC_{50}\ for\ drug\ alone}$$

The values of FIC_{50} for drugs A and B in each combination were used to plot isobologram, a graphical representation of drug–drug interactions. Each data point on such a graph connects the FIC_{50} of drug A on the X axis to FIC_{50} of drug B on the Y axis. Addition of the two FIC_{50} values for each data point provides ΣFIC_{50} for specific combinations. A diagonal connecting FIC = 1 on each axis then allows one to see the significance of each point: $\Sigma FIC_{50} = <1$: Synergy, $\Sigma FIC_{50} = \geq 1$ to <2: Additive, $\Sigma FIC_{50} = \geq 2$ to <4: slight antagonism, $\Sigma FIC_{50} = \geq 4$: strong antagonism [83,84].

4.7. Microscopic evaluation and SYBR Green I assay of the kinetics of stage specific inhibition of growth of P. falciparum by individual drugs and drugs in combination

In order to find if there was stage specificity in the action of **9** alone or combination with antimalarial drugs, highly synchronized *Pf*INDO cultures at ring (R), trophozoite (T), and schizont (S) stages were treated with **9**, antimalarial drugs (**CQ**, **ART**) and synergy combinations of two drugs at their respective IC_{100}. The assay was done in two sets of triplicates, one each for Giemsa stain and SYBR Green assay. Drug pressures were maintained over 48, 24, and 8 h

for ring, trophozoite, and schizonts stages respectively, following which the drugs were removed by media wash and the cultures were maintained in drug free complete RPMI medium for 48 h. For studying the kinetics of the effects of drugs alone and drug combinations, *Pf*INDO ring stage cultures were treated with IC_{100} for 6, 24 and 48 h. Similarly, trophozoite stage cultures were treated with IC_{100} for 18 and 24 h. After the respective incubation periods, drug pressure was removed by media wash and the cultures were maintained under normal culture conditions for a total of 96 h in each case. Percentage of stage-specific inhibition of each treatment was calculated in comparison to drug free control by microscopic counting of 3000 cells for each stage and independently assessed for growth by SYBR Green I fluorescence assay as described earlier. Parasitized and non-parasitized cells were counted by using *Plasmodium* auto count 0.1 software developed by Ma et al. [85]. The parasites with pycnotic morphology were considered as nonviable cells.

4.8. Determination of DNA fragmentation and mitochondrial membrane potential ($\Delta\Psi m$) in P. falciparum

Hoechst 33342 (2′-[4-ethoxyphenyl]-5-[4-methyl-1-piperazinyl]-2,5′-bis-1H-benzimidazole trihydrochloride trihydrate, Invitrogen) was used to detect DNA fragmentation and chromatin condensation in *P. falciparum*. Likewise *P. falciparum* mitochondrial membrane potential ($\Delta\Psi m$) was determined by JC-1 dye (5,5′,6,6′-tetrachloro-1,1′,3,3′-tetraethylbenzimidazolylcarbocyanine iodine, Invitrogen). Briefly, *Pf*3D7 ring stage cultures were treated with IC_{100} of **9** for 12, 24, and 48 h. Similarly, trophozoite stage cultures were treated with IC_{100} for 6, 12 and 24 h. The treated and untreated parasites were incubated with Hoechst 33342 stain for 10 min at room temperature. Similarly, the treated and untreated parasites were incubated with JC-1 dye for 20 min at 37 °C. Then the parasites were washed with PBS and wet mounts of stained cultures were prepared. The slides were observed by using a fluorescence microscope (Nikon 50i).

4.9. Physicochemical parameter calculation of allylated chalcones (**1–42**)

Absorption (%ABS) was calculated by: $\%ABS = 109 - (0.345 \times TPSA)$ [86]. Polar surface area (TPSA) [70–72,79], miLog*P*, number of rotable bonds, and violations of Lipinski's rule of five [86] were calculated using Molinspiration online property calculation toolkit [79]. Aqueous solubility of the compounds was determined using VCC lab online calculation toolkit [87].

Funding

We graciously acknowledge Department of Science and Technology, New Delhi, India (Vide Grant No. SR/S1/OC-16/2008) for financial support.

Transparency declarations

The authors declare no conflict of interest.

Acknowledgments

The authors gratefully acknowledge the Directors of CSIR-IHBT, Palampur, CSIR-CDRI,Lucknow,India and, ICGEB, New Delhi, India for their kind encouragement as well as providing infrastructure for conducting the above work. N.S., U.K.S. and R.K. are indebted to CSIR, New Delhi for Research fellowships. D.M thanks ICMR, New Delhi for Senior Research fellowship and Naveen Kumar Kaushik for thoughtful discussions. D.M. and D.S. thank MR4 who generously provided the chloroquine resistant Dd2 and INDO strains used in the study. Thanks are extended to David Walliker and X. Su who deposited these strains with MR4. We are thankful to S. Kumar for technical support regarding NMR spectra and HRMS recordings.

Appendix A. Supplementary data

Supplementary data related to this article can be found at http://dx.doi.org/10.1016/j.ejmech.2014.03.079.

References

[1] R.P. Tripathi, R.C. Mishra, N. Dwivedi, N. Tewari, S.S. Verma, Current status of malarial control, Current Medicinal Chemistry 12 (2005) 2643–2659.
[2] R.S. Phillips, Current status of malaria and potential for control, Clinical Microbiology Reviews 14 (2001) 208–226.
[3] W.H. Wernsdorfer, The development and spread of drug-resistant malaria, Parasitology Today 7 (1991) 297–303.
[4] G.E.G. Liñares, J.B. Rodriguez, Current status and progresses made in malaria chemotherapy, Current Medicinal Chemistry 14 (2007) 289–314.
[5] D.J. Newman, G.M. Cragg, K.M. Snader, Natural products as sources of new drugs over the period 1981–2002, Journal of Natural Products 66 (2003) 1022–1037.
[6] D.H. Rogers, S.E. Randolph, The global spread of malaria in a future, warmer world, Science 289 (2000) 1763–1766.
[7] P.J. de Vries, T.K. Dien, Clinical pharmacology and therapeutic potential of artemisinin and its derivatives in the treatment of malaria, Drugs 52 (1996) 818–836.
[8] C.J. Woodrow, R.K. Haynes, S. Krishna, Artemisinins, Postgraduate Medical Journal 81 (2005) 71–78.
[9] R.N. Price, F. Nosten, C. Luxemburger, M. van Vugt, L. Phaipun, T. Chongsuphajaisiddhi, N.J. White, Artesunate/mefloquine treatment of multi-drug resistant *falciparum* malaria, Transactions of the Royal Society of Tropical Medicine and Hygiene 91 (1997) 574–577.
[10] S.R. Meshnick, Artemisinin: mechanisms of action, resistance and toxicity, International Journal of Parasitology 32 (2002) 1655–1660.
[11] A.M. Dondorp, F. Nosten, P. Yi, D. Das, A.P. Phyo, J. Tarning, K.M. Lwin, F. Ariey, W. Hanpithakpong, S.J. Lee, P. Ringwald, K. Silamut, M. Imwong, K. Chotivanich, P. Lim, T. Herdman, S.S. An, S. Yeung, P. Singhasivanon, N.P.J. Day, N. Lindegardh, D. Socheat, N.J. White, Artemisinin resistance in *Plasmodium falciparum* malaria, New England Journal of Medicine 361 (2009) 455–467.
[12] C. Luxemburger, A. Brockman, K. Silamut, F. Nosten, M. van Vugt, F. Gimenez, T. Chongsuphajaisiddhi, N.J. White, Two patients with falciparum malaria and poor *in vivo* responses to artesunate, Transactions of the Royal Society of Tropical Medicine and Hygiene 92 (1998) 668–669.
[13] A.P. Alker, P. Lim, R. Sem, N.K. Shah, P. Yi, D.M. Bouth, R. Tsuyuoka, J.D. Maguire, T. Fandeur, F. Ariey, C. Wongsrichanalai, S.R. Meshnick, P*f*mdr1 and *in vivo* resistance to artesunate-mefloquine in falciparum malaria on the Cambodian-Thai border, American Journal of Tropical Medicine and Hygiene 76 (2007) 641–647.
[14] M. Enserink, Malaria: signs of drug resistance rattle experts, trigger bold plan, Science 322 (2008) 1776.
[15] World Health Organization, The Use of Artemisinin and Its Derivatives as Anti-Malarial Drugs, in: Report of a Joint CTD/DMP/TDR Informal Consultation, 1998, 10–12 June, Geneva.
[16] V.K. Bhasin, L. Nair, Act now—with caution—for malaria treatments, Lancet Infectious Diseases 3 (2003) 609.
[17] S. Takala-Harrison, T.G. Clark, C.G. Jacob, M.P. Cummings, O. Miotto, A.M. Dondorp, M.M. Fukuda, F. Nosten, H. Noedl, M. Imwong, D. Bethell, Y. Se, C. Lon, S.D. Tyner, D.L. Saunders, D. Socheat, F. Ariey, A.P. Phyo, P. Starzengruber, H.P. Fuehrer, P. Swoboda, K. Stepniewska, J. Flegg, C. Arze, G.C. Cerqueira, J.C. Silva, S.M. Ricklefs, S.F. Porcella, R.M. Stephens, M. Adams, L.J. Kenefic, S. Campino, S. Auburn, B. MacInnis, D.P. Kwiatkowski, X. Su, N.J. White, P. Ringwald, C.V. Plowe, Genetic loci associated with delayed clearance of *Plasmodium falciparum* following artemisinin treatment in Southeast Asia, Proceedings of the National Academy of Sciences 110 (2013) 240–245.
[18] E.M. Guantai, K. Ncokazi, T.J. Egan, J. Gut, P.J. Rosenthal, R. Bhampidipati, A. Kopinathan, P.J. Smith, K. Chibale, Enone- and chalcone-chloroquinoline hybrid analogues: *In silico* guided design, synthesis, antiplasmodial activity, *in vitro* metabolism, and mechanistic studies, Journal of Medicinal Chemistry 54 (2011) 3637–3649.
[19] M. Chen, T.G. Theander, S.B. Christensen, L. Hviid, L. Zhai, A. Kharazmi, Licochalcone A, a new antimalarial agent, inhibits in vitro growth of the human malaria parasite *Plasmodium falciparum* and protects mice from *P. yoelii* infection, Antimicrobial Agents and Chemotherapy 38 (1994) 1470–1475.
[20] A. Yenesew, M. Duli, S. Derese, J.O. Midiwo, M. Heydenreich, M.G. Peter, H. Akala, J. Wangui, P. Liyala, N.C. Waters, Anti-plasmodial flavonoids from the stem bark of *Erythrina abyssinica*, Phytochemistry 65 (2004) 3029–3032.

[21] T. Narender, T.K. Shweta, M.S. Rao, K. Srivastava, S.K. Puri, Prenylated chalcones isolated from *Crotalaria* genus inhibits *in vitro* growth of the human malaria parasite *Plasmodium falciparum*, Bioorganic & Medicinal Chemistry Letters 15 (2005) 2453–2455.

[22] J.F. Stevens, J.E. Page, Xanthohumol and related prenylflavonoids from hops and beer: to your good health, Phytochemistry 65 (2004) 1317–1330.

[23] M. Chen, S.B. Christensen, L. Zhai, M.H. Rasmussen, T.G. Theander, S. Frøkjaer, B. Steffansen, J. Davidsen, A. Kharazmi, The novel oxygenated chalcone, 2,4-Dimethoxy-4'-butoxychalcone, exhibits potent activity against human malaria parasite *Plasmodium falciparum in vitro* and rodent parasites *Plasmodium berghei* and *Plasmodium yoelii in vivo*, Journal of Infectious Diseases 176 (1997) 1327–1333.

[24] J.N. Dominguez, C. Leon, J. Rodrigues, N.G. De Dominguez, J. Gut, P.J. Rosenthal, Synthesis and evaluation of new antimalarial phenylurenyl chalcone derivatives, Journal of Medicinal Chemistry 48 (2005) 3654–3658.

[25] R. Li, G.L. Kenyon, F.E. Cohen, X.W. Chen, B.Q. Gong, J.N. Dominguez, E. Davidson, G. Kurzban, R.E. Miller, E.O. Nuzum, *In vitro* antimalarial activity of chalcones and their derivatives, Journal of Medicinal Chemistry 38 (1995) 5031–5037.

[26] M. Liu, P. Wilairat, M.L. Go, Antimalarial alkoxylated and hydroxylated chalcones: structure-activity relationship analysis, Journal of Medicinal Chemistry 44 (2001) 4443–4452.

[27] M.L. Go, M. Liu, P. Wilairat, P.J. Rosenthal, K.J. Saliba, K. Kirk, Antiplasmodial chalcones inhibit sorbitol-induced hemolysis of *Plasmodium falciparum* infected erythrocytes, Antimicrobial Agents and Chemotherapy 48 (2004) 3241–3245.

[28] V. Tomar, G. Bhattacharjee, Kamaluddin, S. Rajakumar, K. Srivastava, S.K. Puri, Synthesis of new chalcone derivatives containing acridinyl moiety with potential antimalarial activity, European Journal of Medicinal Chemistry 45 (2010) 745–751.

[29] X. Wu, P. Wilairat, M.L. Go, Antimalarial activity of ferrocenyl chalcones, Bioorganic & Medicinal Chemistry Letters 12 (2002) 2299–2302.

[30] M. Maitrejean, G. Comte, D. Barron, K. El Kirat, G. Conseil, A. Di Pietro, The flavanolignan silybin and its hemisynthetic derivatives, a novel series of potential modulators of *p*-glycoprotein, Bioorganic & Medicinal Chemistry Letters 10 (2000) 157–160.

[31] M.C. Henderson, C.L. Miranda, J.F. Stevens, M.L. Deinzer, D.R. Buhler, *In vitro* inhibition of human P450 enzymes by prenylated flavonoids from hops, *Humulus lupulus*, Xenobiotica 30 (2000) 235–251.

[32] S.R. Milligan, J.C. Kalita, V. Pocook, V. Van de Kauter, J.F. Stevens, M.L. Deinzer, H. Rong, D. De Keukeleire, The endocrine activities of 8-prenylnaringenin and related hop (*Humulus lupulus* L.) flavonoids, Journal of Clinical Endocrinology & Metabolism 85 (2000) 4912–4915.

[33] C.L. Miranda, G.L. Aponso, J.F. Stevens, M.L. Deinzer, D.R. Buhler, Prenylated chalcones and flavanones as inducers of quinone reductase in mouse Hepa 1c1c7 cells, Cancer Letters 149 (2000) 21–29.

[34] (a) R.H. Hans, E.M. Guantai, C. Lategan, P.J. Smith, B. Wan, S.G. Franzblau, J. Gut, P.J. Rosenthal, K. Chibale, Synthesis, antimalarial and antitubercular activity of acetylenic chalcones, Bioorganic & Medicinal Chemistry Letters 20 (2010) 942–944;
(b) N. Tadigoppula, V. Korthikunta, S. Gupta, P. Kancharla, T. Khaliq, A. Soni, R.K. Srivastave, K. Srivastava, S.K. Puri, K.S.R. Raju, Wahajuddin, P.S. Sijwali, V. Kumar, I.M. Mohammad, Journal of Medicinal Chemistry 56 (2013) 31–45.

[35] P.T. Anastas, J.C. Warner, Green Chemistry: Theory and Practice, Oxford University Press, New York, 1998, p. 30.

[36] Besides a large number of medicinal and biological activities, natural products are also significant source of inspiration for the design of value added products. In this context, vanillin (4-hydroxy-3-methoxybenzaldehyde) [37a,b] is one the most widespread compounds in the plant kingdom and is widely used as flavor compound in food and cosmetics with an estimated annual worldwide consumption of synthetic vanillin more than 200 tons. Further, vanillin displays antimicrobial, anticancer and antioxidant activities besides it has been used as a natural synthon in the production of fine chemicals, cationic surfactants [37b], other flavoring molecules and bioactive compounds [37c] including some drugs such as Aldomet, L-dopa and trimethaprim. Hence, vanillin was decided to explore as a core structure for the concise and economical synthesis of allylated chalcones for their improved antimalarial activity without violating Lipinski's parameters.

[37] (a) A.K. Sinha, U.K. Sharma, N. Sharma, A comprehensive review on vanilla flavor: extraction, isolation and quantification of its chemical constituents, International Journal of Food Sciences and Nutrition 9 (2008) 299–326;
(b) N.J. Walton, M.J. Mayer, A. Narbad, Molecules of interest-vanillin, Phytochemistry 63 (2003) 505–515;
(c) N. Negm, N.G. Kandile, M.A. Mohamad, Synthesis, characterization and surface activity of new eco-friendly Schiff bases vanillin derived cationic surfactants, Journal of Surfactants and Detergents 14 (2011) 325–331;
(d) S.T. Harini, H.V. Kumar, J. Rangaswamy, N. Naik, Synthesis, antioxidant and antimicrobial of novel vanillin derived piperidin-4-one oxime esters: preponderant role of the phenyl ester substituents on the piperidin-4-one oxime core, Bioorganic & Medicinal Chemistry Letters 22 (2012) 7588–7592.

[38] B. Xu, H. Pelish, T. Kirchhausen, G.B. Hammond, Large scale synthesis of the Cdc42 inhibitor secramine A and its inhibition of cell spreading, Organic & Biomolecular Chemistry 4 (2006) 4149–4157.

[39] S. Vogel, J. Heilmann, Synthesis, cytotoxicity, and antioxidative activity of minor prenylated chalcones from *Humulus lupulus*, Journal of Natural Products 71 (2008) 1237–1241.

[40] J.C. Aponte, M. Verástegui, E. Málaga, M. Zimic, M. Quiliano, A.J. Vaisberg, R.H. Gilman, G.B. Hammond, Synthesis, cytotoxicity, and anti-*Trypanosoma cruzi* activity of new chalcones, Journal of Medicinal Chemistry 51 (2008) 6230–6234.

[41] B. Srinivasan, T.E. Johnson, R. Lad, C. Xing, Structure-activity relationship studies of chalcone leading to 3-hydroxy-4,3',4',5'-tetramethoxychalcone and its analogues as potent nuclear factor KB inhibitors and their anticancer activities, Journal of Medicinal Chemistry 52 (2009) 7228–7235.

[42] M. Cabrera, M. Simoens, G. Falchi, M.L. Lavaggi, O.E. Piro, E.E. Castellano, A. Vidal, A. Azqueta, A. Monge, L.A. de Cerain, G. Sagrera, G. Seoane, H. Cerecetto, M. Gonzalez, Synthetic chalcones, flavanones, and flavones as antitumoral agents: biological evaluation and structure-activity relationships, Bioorganic & Medicinal Chemistry 15 (2007) 3356–3367.

[43] A. Boumendjel, J. Boccard, P.A. Carrupt, E. Nicolle, M. Blanc, A. Geze, L. Choisnard, D. Wouessidjewe, E.L. Matera, C. Dumontet, Antimitotic and antiproliferative activities of chalcones: forward structure-activity relationship, Journal of Medicinal Chemistry 51 (2008) 2307–2310.

[44] A.G. Mehta, A.A. Patel, Studies on novel *N*4-[4,6-Diaryl-2-pyrimidinyl]-7-chloro-4-quinolinamine and their microbicidal efficacy, E-Journal of Chemistry 6 (2009) S406–S412. http://www.e-journals.net.

[45] A. Lévai, Synthesis of chlorinated 3,5-diaryl-2-pyrazolines by the reaction of chlorochalcones with hydrazines, ARKIVOC (ix) (2005) 344–352.

[46] S.K.A. Rahaman, Y.R. Pasad, P. Kumar, B. Kumar, Synthesis and anti-histaminic activity of some novel pyrimidines, Saudi Pharmaceutical Journal 17 (2009) 259–264.

[47] M. Smilkstein, N. Sriwilaijaroen, J.X. Kelly, P. Wilairat, M. Riscoe, Simple and inexpensive fluorescence-based technique for high throughput antimalarial drug screening, Antimicrobial Agents and Chemotherapy 48 (2004) 1803–1806.

[48] N. Mishra, P. Arora, B. Kumar, L.C. Mishra, A. Bhattacharya, S.K. Awasthi, V.K. Bhasin, Synthesis of novel substituted 1,3-diaryl propenone derivatives and their antimalarial activity *in vitro*, European Journal of Medicinal Chemistry 43 (2008) 1530–1535.

[49] S. Manohar, S.I. Khan, D.S. Rawat, Synthesis, antimalarial activity and cytotoxicity of 4-aminoquinoline–triazine conjugates, Bioorganic & Medicinal Chemistry Letters 20 (2010) 322–325.

[50] S.J. Kesten, M.J. Degnan, J. Hung, D.J. McNamara, D.F. Ortwine, S.E. Uhlendorf, L. Werbel, Antimalarial drugs. Synthesis and antimalarial properties of 1-imino derivatives of 7-chloro-3-substituted-3,4-dihydro-1,9(2*H*,10*H*)-acridinediones and related structures, Journal of Medicinal Chemistry 35 (1992) 3429–3447.

[51] S. Fu, S.H. Xiao, Pyronaridine: a new antimalarial drug, Parasitology Today 7 (1991) 310–313.

[52] M. Liu, P. Wilairat, S.L. Croft, A.L.C. Tan, M.L. Go, Structure–activity relationships of antileishmanial and antimalarial chalcones, Bioorganic & Medicinal Chemistry 11 (2003) 2729–2738.

[53] R. Kumar, D. Mohanakrishnan, A. Sharma, N.K. Kaushik, K. Kalia, A.K. Sinha, D. Sahal, Reinvestigation of structure-activity relationship of methoxylated chalcones as antimalarials: synthesis and evaluation of 2,4,5-trimethoxy substituted patterns as lead candidates derived from abundantly available natural β-asarone, European Journal of Medicinal Chemistry 45 (2010) 5292–5301.

[54] J.C. Trivedi, J.B. Bariwal, K.D. Upadhyay, Y.T. Naliapara, S.K. Joshi, C.C. Pannecouque, E. De Clercq, A.K. Shah, Improved and rapid synthesis of new coumarinyl chalcone derivatives and their antiviral activity, Tetrahedron Letters 48 (2007) 8472–8474.

[55] G. Sandeep, Y.S. Ranganath, S. Bhasker, N. Rajkumar, Synthesis and biological screening of some novel coumarin derivatives, Asian Journal of Research in Chemistry 2 (2009) 46–48.

[56] K. Kaur, M. Jain, R.P. Reddy, R. Jain, Quinolines and structurally related heterocycles as antimalarials, European Journal of Medicinal Chemistry 45 (2010) 3245–3264.

[57] T.J. Egan, R. Hunter, C.H. Kinchella, H.M. Marques, A. Misplon, J.C. Walden, Structure-function relationships in aminoquinolines: effect of amino and chloro groups on quinoline–hematin complex formation, inhibition of β-hematin formation and antiplasmodial activity, Journal of Medicinal Chemistry 43 (2000) 283–291.

[58] R.H. Wiley, in: A. Weissberger (Ed.), Pyrazoles, Pyrazolines, Pyrazolidines, Indazoles and Condensed Rings: The Chemistry of Heterocyclic Compounds, vol. 22, Interscience Publishers, New York, 1967, p. 180.

[59] B. Witkowski, J.J. Lelievre, M.J.L. Barraga'n, V.V. Laurent, X.-Z. Su, A. Berry, F. Benoit-Vical, Increased tolerance to artemisinin in *Plasmodium falciparum* is mediated by a quiescence mechanism, Antimicrobial Agents and Chemotherapy 54 (2010) 1872–1877.

[60] J. Wang, L. Huang, J. Li, Q. Fan, Y. Long, Y. Li, B. Zhou, Artemisinin directly targets malarial mitochondria through its specific mitochondrial activation, PLoS ONE 5 (2010) e9582.

[61] A. Bell, Antimalarial drug synergism and antagonism: mechanistic and clinical significance, FEMS Microbiology Letters 253 (2005) 171–184.

[62] N. Vyas, B.A. Avery, M.A. Avery, C.M. Wyandt, Carrier-mediated partitioning of artemisinin into *Plasmodium falciparum*-infected erythrocytes, Antimicrobial Agents and Chemotherapy 46 (2002) 105–109.

[63] M.L. Lopez, R. Vommaro, M. Zalis, W. Souza, S. Blair, C. Segura, Induction of cell death on *Plasmodium falciparum* asexual blood stages by *Solanum nudum* steroids, Parasitology International 59 (2010) 217–225.
[64] P.R. Totino, C.T. Daniel-Ribeiro, S. Corte-Real, F.C.M. de Fátima, *Plasmodium falciparum*: erythrocytic stages die by autophagic-like cell death under drug pressure, Experimental Parasitology 118 (2008) 478–486.
[65] F. Belloc, P. Dumain, M.R. Boisseau, C. Jalloustre, J. Reiffers, P. Bernard, F. Lacombe, A flow cytometric method using Hoechst 33342 and propidium iodide for simultaneous cell cycle analysis and apoptosis determination in unfixed cells, Cytometry 17 (1994) 59–65.
[66] N. Sharma, D. Mohanakrishnan, A. Shard, A. Sharma, Saima, A.K. Sinha, D. Sahal, Stilbene–chalcone hybrids: design, synthesis, and evaluation as a new class of antimalarial scaffolds that trigger cell death through stage specific apoptosis, Journal of Medicinal Chemistry 55 (2012) 297–311.
[67] L.L. Chat, R.E. Sinden, J.T. Dessensa, The role of metacaspase 1 in *Plasmodium berghei* development and apoptosis, Molecular and Biochemical Parasitology 153 (2007) 41–47.
[68] S.C. Arambage, K.M. Grant, I. Pardo, L.R. Cartwright, H. Hurd, Malaria ookinetes exhibit multiple markers for apoptosis-like programmed cell death *in vitro*, Parasites & Vectors 2 (2009) 32.
[69] A. Rennenberg, C. Lehmann, A. Heitmann, T. Witt, G. Hansen, K. Nagarajan, C. Deschermeier, V. Turk, R. Hilgenfeld, V.T. Heussler, Exoerythrocytic *Plasmodium* parasites secrete a cysteine protease inhibitor involved in sporozoite invasion and capable of blocking cell death of host hepatocytes, PLoS Pathogens 6 (2010) e1000825.
[70] P. Ertl, B. Rohde, P. Selzer, Fast calculation of molecular polar surface area as a sum of fragment based contributions and its application to the prediction of drug transport properties, Journal of Medicinal Chemistry 43 (2000) 3714–3717.
[71] R. Mannhold, G.I. Poda, C. Ostermann, I.V. Tetko, Calculation of molecular lipophilicity: state-of-the-art and comparison of logP methods on more than 96,000 compounds, Journal of Pharmaceutical Sciences 98 (2009) 861–893.
[72] S. Rajasekaran, G.K. Rao, P.N.S. Pai, A. Ranjan, Design, synthesis, antibacterial and *in vitro* antioxidant activity of substituted 2*H* benzopyran-2-one derivatives, International Journal of ChemTech Research 3 (2011) 555–559.
[73] D.B. Kassel, Applications of high-throughput ADME in drug discovery, Current Opinion in Chemical Biology 8 (2004) 339–345.
[74] M.S. Alavijeh, M. Chishty, M.Z. Qaiser, A.M. Palmer, Drug metabolism and pharmacokinetics, the blood-brain barrier and central nervous system drug discovery, Journal of the American Society for Experimental NeuroTherapeutics 2 (2005) 554–571.
[75] C.A.S. Bergström, *In silico* predictions of drug solubility and permeability: two rate-limiting barriers to oral drug absorption, Basic & Clinical Pharmacology & Toxicology 96 (2005) 156–161.
[76] I.V. Tetko, I. Jaroszewicz, J.A. Platts, J. Kuduk-Jaworska, Calculation of lipophilicity for Pt (II) complexes: experimental comparison of several methods, Journal of Inorganic Biochemistry 102 (2008) 1424–1437.
[77] V.N. Viswanadhan, A.K. Ghose, J.J. Wendoloski, Estimating aqueous solvation and lipophilicity of small organic molecules: a comparative overview of atom/group contribution methods, Perspectives in Drug Discovery and Design 19 (2000) 85–98.
[78] Y. Zhao, M.H. Abraham, J. Lee, A. Hersey, N.C. Luscombe, G. Beck, B. Sherborne, I. Cooper, Rate-limited steps of human oral absorption and QSAR studies, Pharmaceutical Research 19 (2002) 1446–1457.
[79] Molinspiration Cheminformatics. http://www.molinspiration.com/servics/properties.html.
[80] W. Trager, J.B. Jensen, Human malaria parasites in continuous culture, Science 193 (1976) 673–675.
[81] C. Lambros, J.P. Vanderberg, Synchronization of *Plasmodium falciparum* erythrocytic stages in culture, Journal of Parasitology 65 (1979) 418–420.
[82] T. Mosmann, Rapid colorimetric assay for cellular growth and survival: application to proliferation and cytotoxicity assays, Journal of Immunological Methods 65 (1983) 55–63.
[83] A. Bhattacharya, L.C. Mishra, M. Sharma, S.K. Awasthi, V.K. Bhasin, Antimalarial pharmacodynamics of chalcone derivatives in combination with artemisinin against *Plasmodium falciparum in vitro*, European Journal of Medicinal Chemistry 44 (2009) 3388–3393.
[84] F.C. Odds, Synergy, antagonism, and what the chequerboard puts between them, Journal of Antimicrobial Chemotherapy 52 (2003) 1.
[85] C. Ma, P. Harrison, L. Wang, R.L. Coppel, Automated estimation of parasitaemia of *Plasmodium yoelii* infected mice by digital image analysis of Giemsa-stained thin blood smears, Malaria Journal 9 (2010) 348.
[86] C.A. Lipinski, F. Lombardo, B.W. Dominy, P.J. Feeney, Experimental and computational approaches to estimate solubility and permeability in drug discovery and development settings, Advanced Drug Delivery Reviews 23 (1997) 3–25.
[87] www.vcclab.org/lab/alogps.